Manuscript ID: RA-ART-07-2015-014079

Revised Supporting information for:

Benzodithieno-imidazole based π-conjugated fluorescent polymer probe for selective sensing of Cu^{2+}

Dipanjan Giri and Sanjib K Patra*

Department of Chemistry, IIT Kharagpur, Kharagpur 721302, WB, INDIA

1. Determination of Quantum yield and Life time:

All the UV−Vis absorption and fluorescence emission spectra were collected using a Shimadzu (model UV 2450) UV−Vis spectrophotometer and a Spex Fluorolog-3 (model FL3−11) spectrofluorimeter, respectively. Throughout all the measurements, the concentration was maintained at ($\sim 2 \times 10^{-5}$) M.

Fluorescence quantum yields were measured with respect to a secondary standard quinine sulphate (λ_{abs}=349 nm) in 0.1 M H_2SO_4 (Φ = 0.57) at 298 K.[1]The following equation was used to calculate the quantum yields:

$$\frac{\Phi_R}{\Phi_S} = \frac{A_S}{A_R} \times \frac{(Abs)_R}{(Abs)_S} \times \frac{\eta_S^2}{\eta_R^2} \quad (1)$$

Here Φ represents the quantum yield, (Abs) represents the absorbance, A represents the area under the fluorescence curve, and η is the refractive index of the medium. $\eta_{DMSO/H2O}$ was calculated using Arago-biot (AB) equation.[2] The subscript S and R denotes the corresponding parameters for the sample and reference, respectively.

Experimental details for TCSPC measurement: The time-resolved emission decays were recorded using a Time-Correlated Single Photon Counting (TCSPC) picoseconds spectrophotometer.[3] The fluorescence decay response of **4b** and **P2** and their coordinated complexes with Cu^{2+} was investigated in DMSO:H_2O. The solution of Cu^{2+} cation was prepared in water and was added to the stock solution of **4b** and **P2** which were prepared in DMSO by maintaining the 1:1 metal ligand ratio. All the samples were excited using a picosecond diode laser at 336 nm (IBH, UK, Nanoled), and the signals were recorded at magic angle (54.71) using a Hamamatsu microchannel plate photomultiplier tube (3809U). The typical instrument response function in our setup is 100 ps. The instrument response function of our setup is ~800 ps. Time-resolved fluorescence decays were analyzed using IBH DAS-6 decay analysis software.

Preparation of thin film for solid state PL measurement:

The quartz substrates (17 x 15 x 1 mm^3) were cleaned in a fresh piranha solution (7:3 mixture of 98% H_2SO_4/30% H_2O_2), washed with Milli-Q water, and followed by ultrasonication in alkaline isopropanol and 0.1 M aqueous HCl at 60^oC for 1 h each. After

careful washing with Milli-Q water, thin film of the polymer **P2** was prepared by spin coating on quartz plate. A solution of **P2** in toluene (~ 3 x 10^{-4}M) was dropped on quartz plate and it was spin coated at 5000 rpm for 60 second followed by 8000 rpm for 120 seconds. PL data pf the polymer film was measured. After that the film was dipped in different concentration of aqueous Cu^{2+} solution for 30 min followed by repetitive and extensive washing (at least 20 times) by Milli-Q water to remove any unbound (free) Cu^{2+} ion. After drying in air, PL response was recorded.

2a. NMR spectra

Fig S1: ^{1}H NMR (400MHz, $CDCl_3$) of **1**

Fig S2: $^{13}C\{^{1}H\}$NMR (100MHz, $CDCl_3$) of **1**

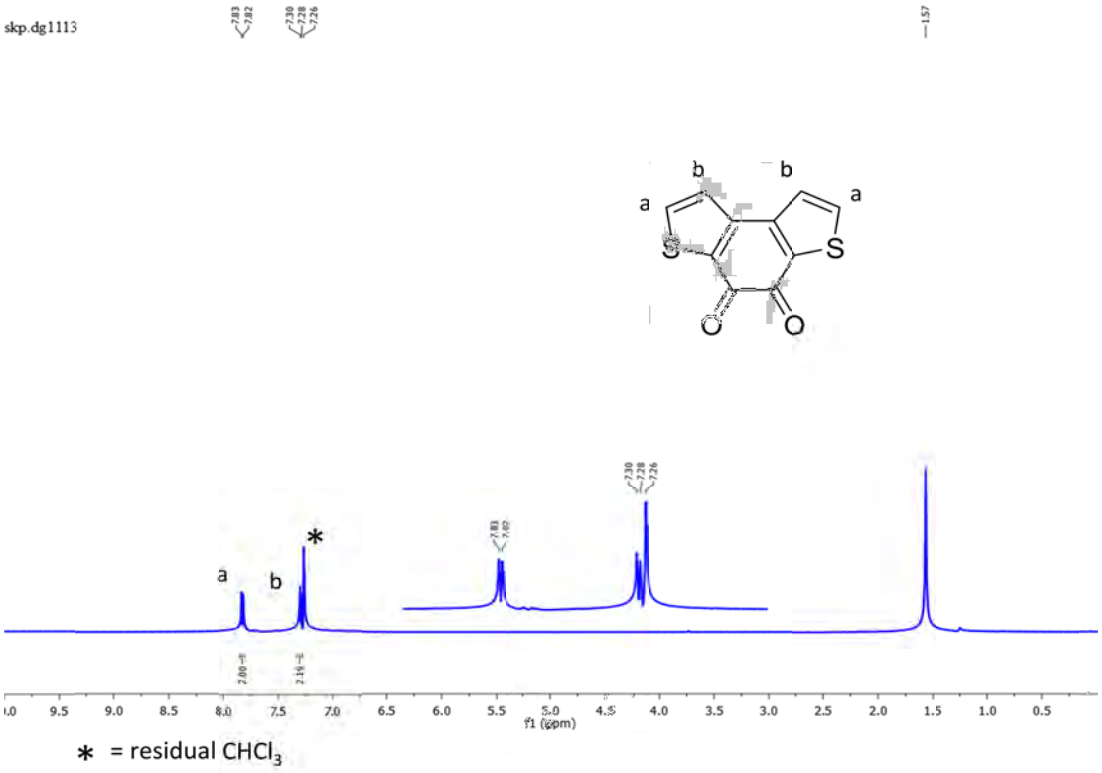

Fig S3: ^{1}H NMR (400MHz, $CDCl_3$) of **2**

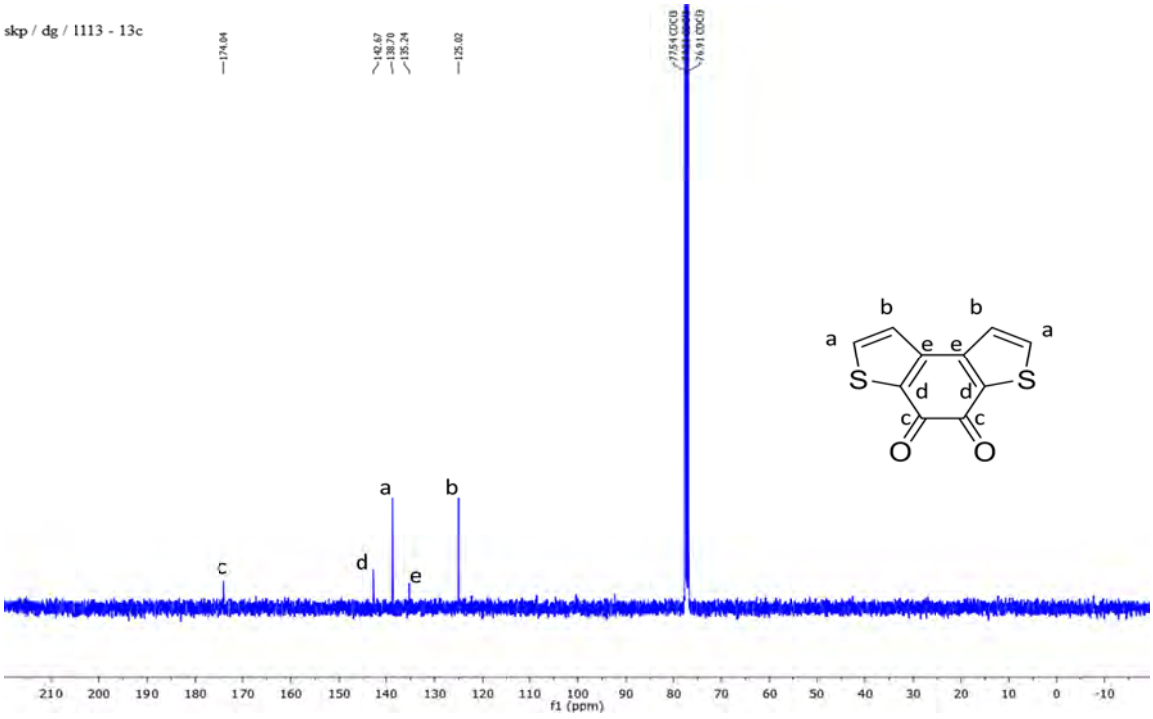

Fig S4: $^{13}C\{^{1}H\}$NMR (100MHz, $CDCl_3$) of **2**

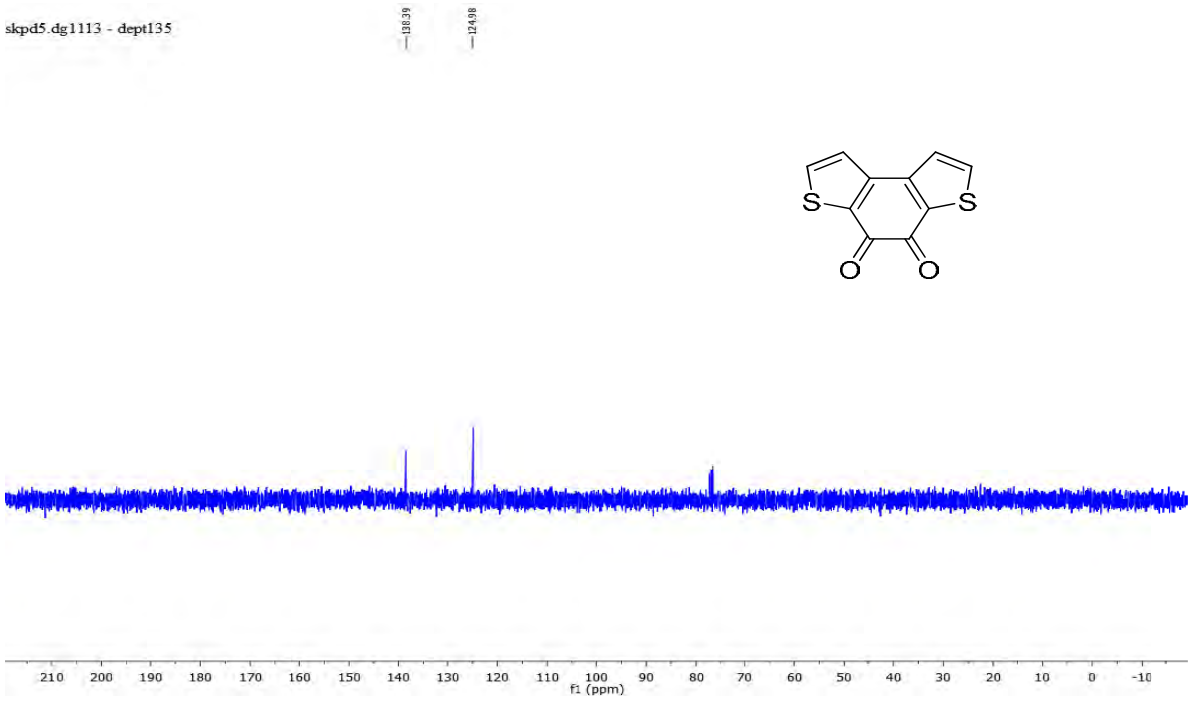

Fig S5: DEPT-135 (100MHz, $CDCl_3$) of **2**

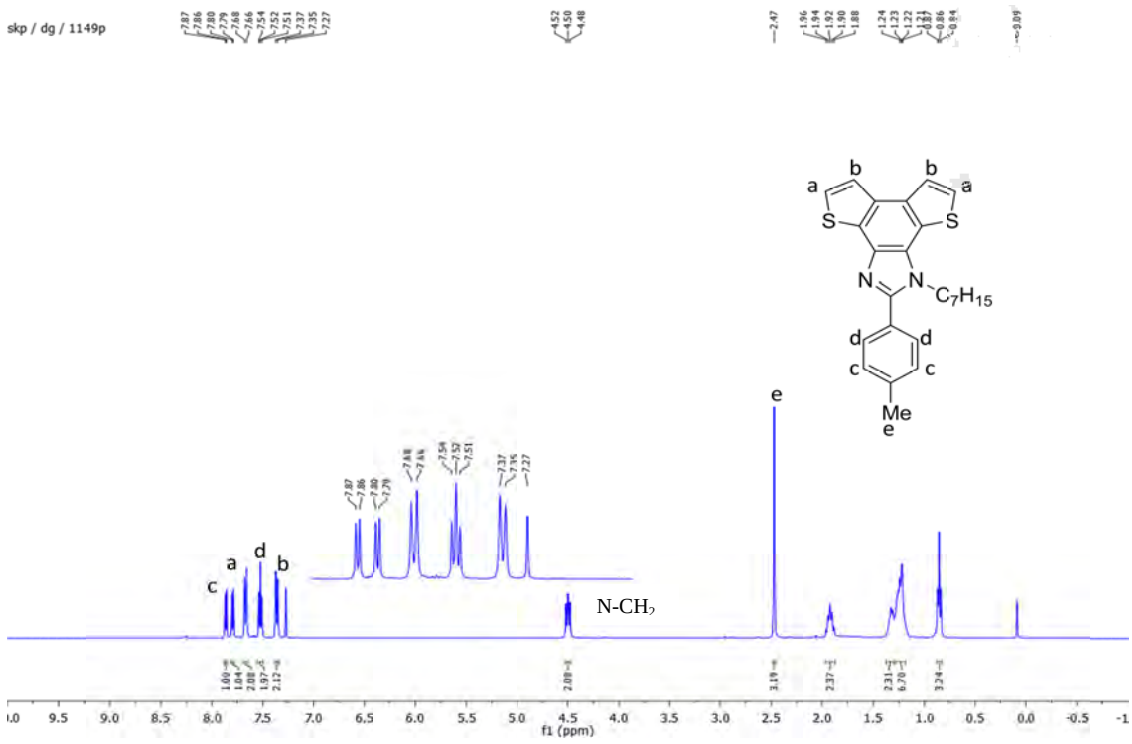

Fig S6: ^{1}HNMR (600MHz, $CDCl_3$) of **4a**

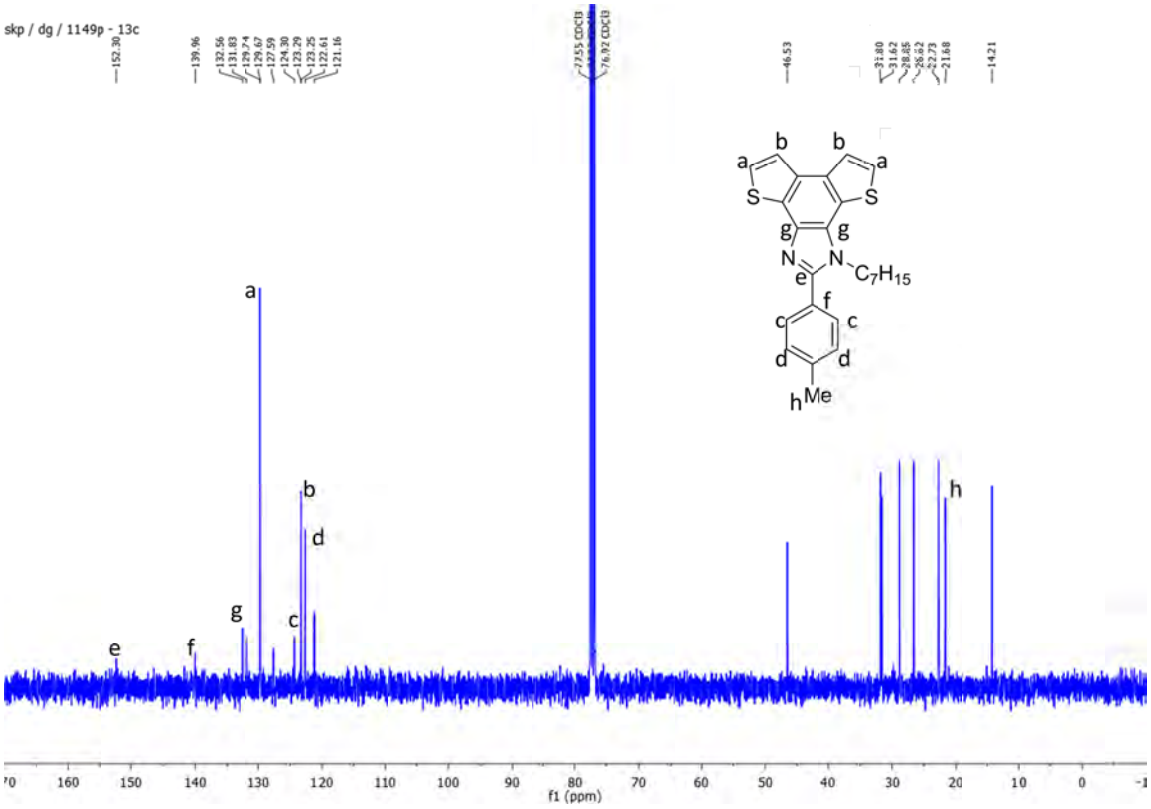

Fig S7: $^{13}C\{^{1}H\}$NMR (150MHz, $CDCl_3$) of **4a**

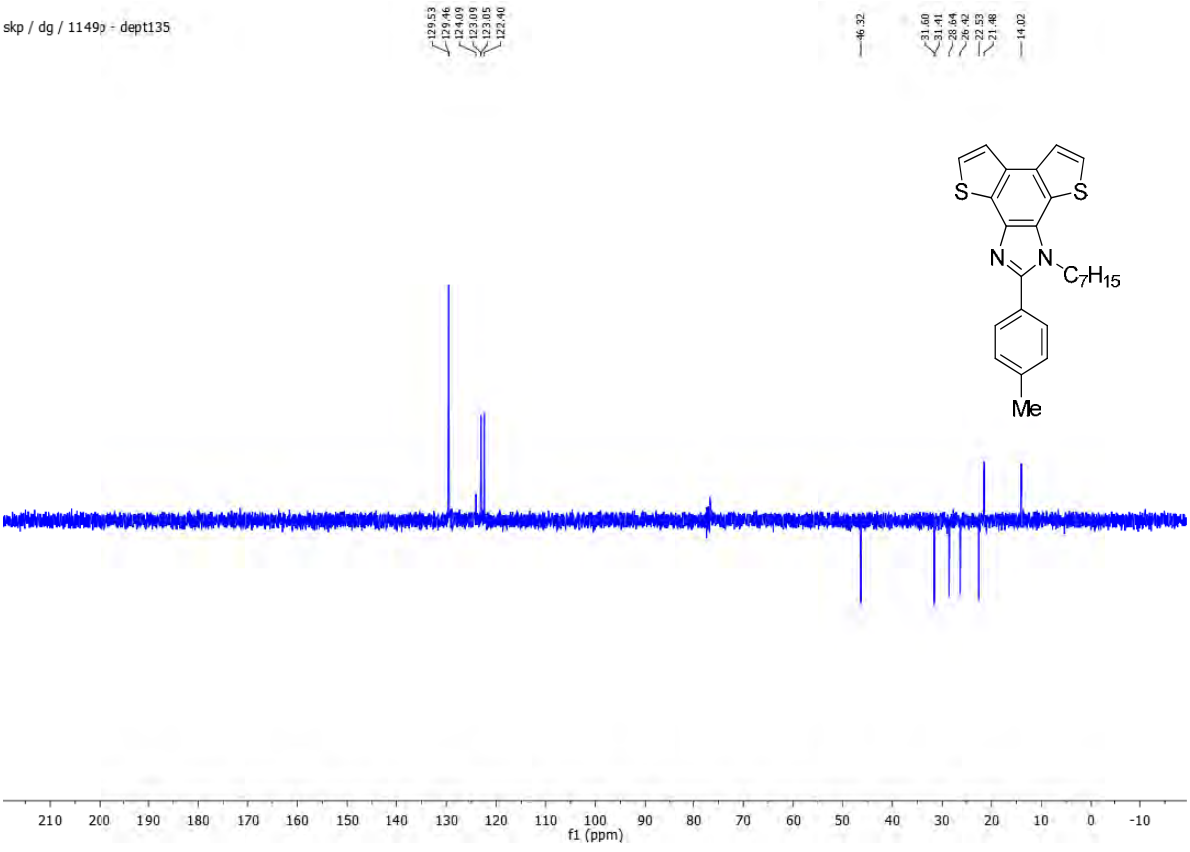

Fig S8: DEPT-135 (150MHz, $CDCl_3$) of **4a**

Fig S9: ^{1}HNMR (600MHz, $CDCl_3$) of **4b**

Fig S10: $^{13}C\{^{1}H\}$NMR (150MHz, $CDCl_3$) of **4b**

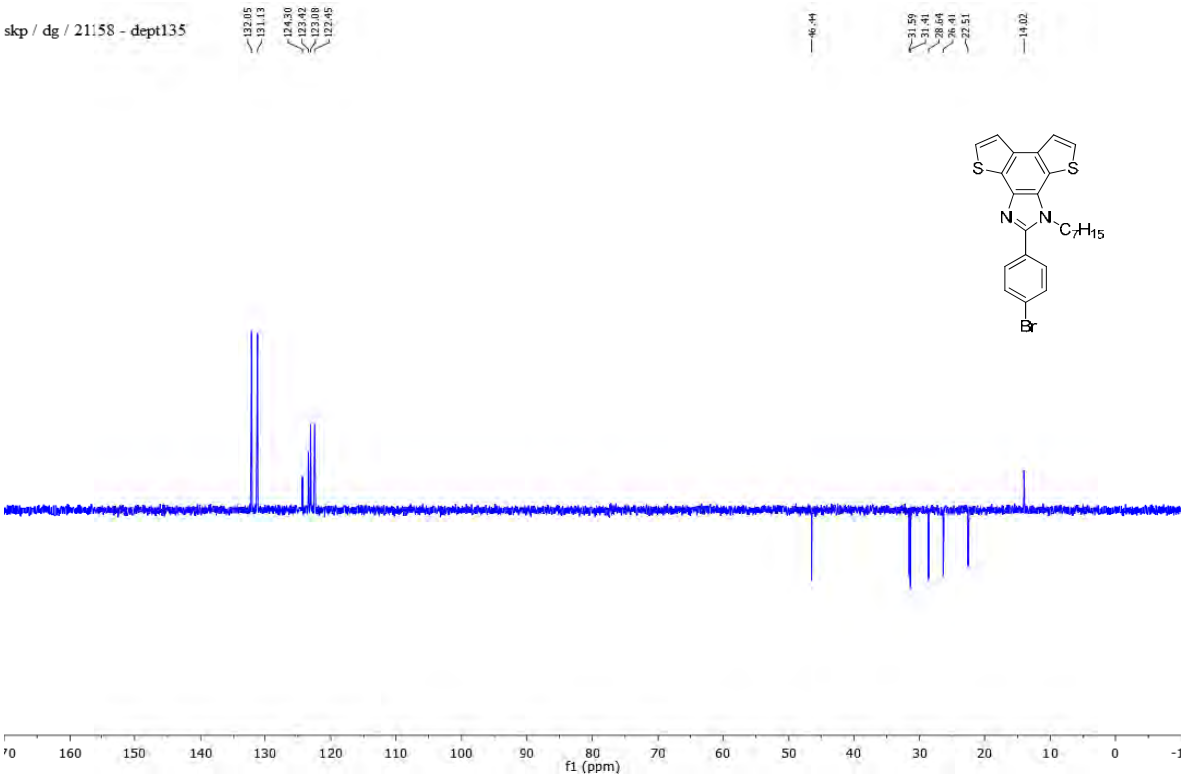

Fig S11: DEPT-135 (150MHz, $CDCl_3$) of **4b**

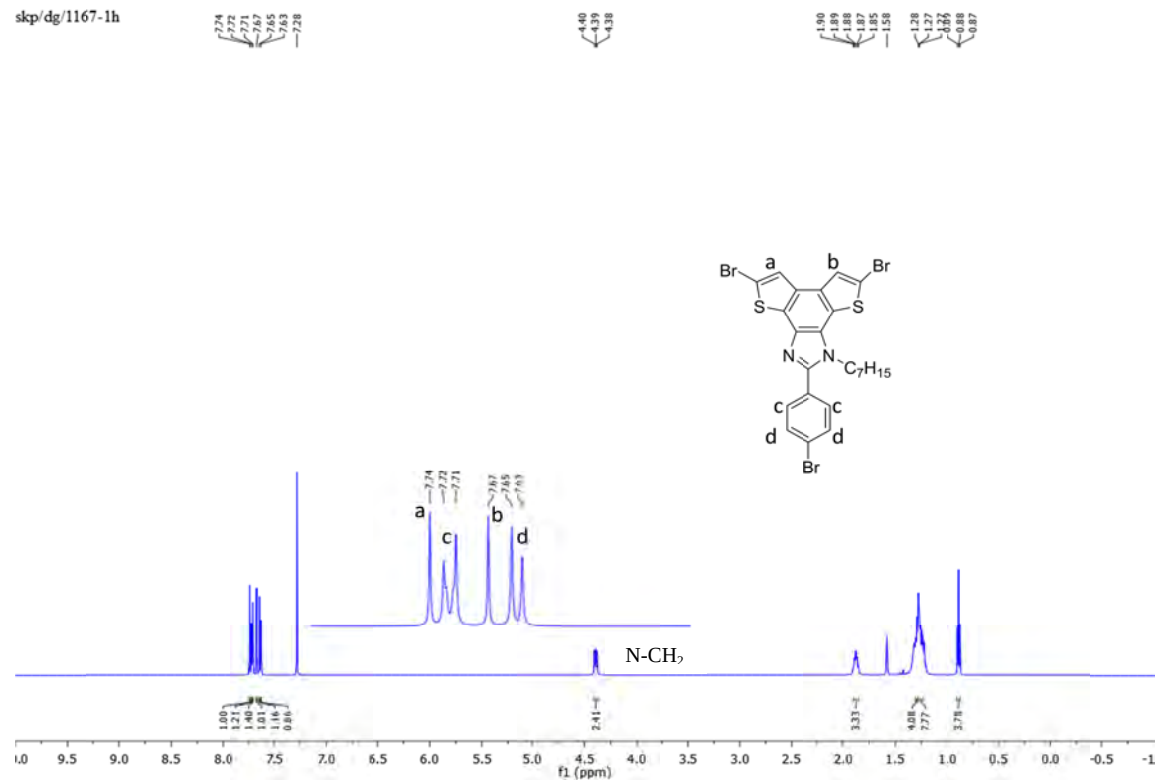

Fig S12: ^1H NMR (600MHz, $CDCl_3$) of **5b**

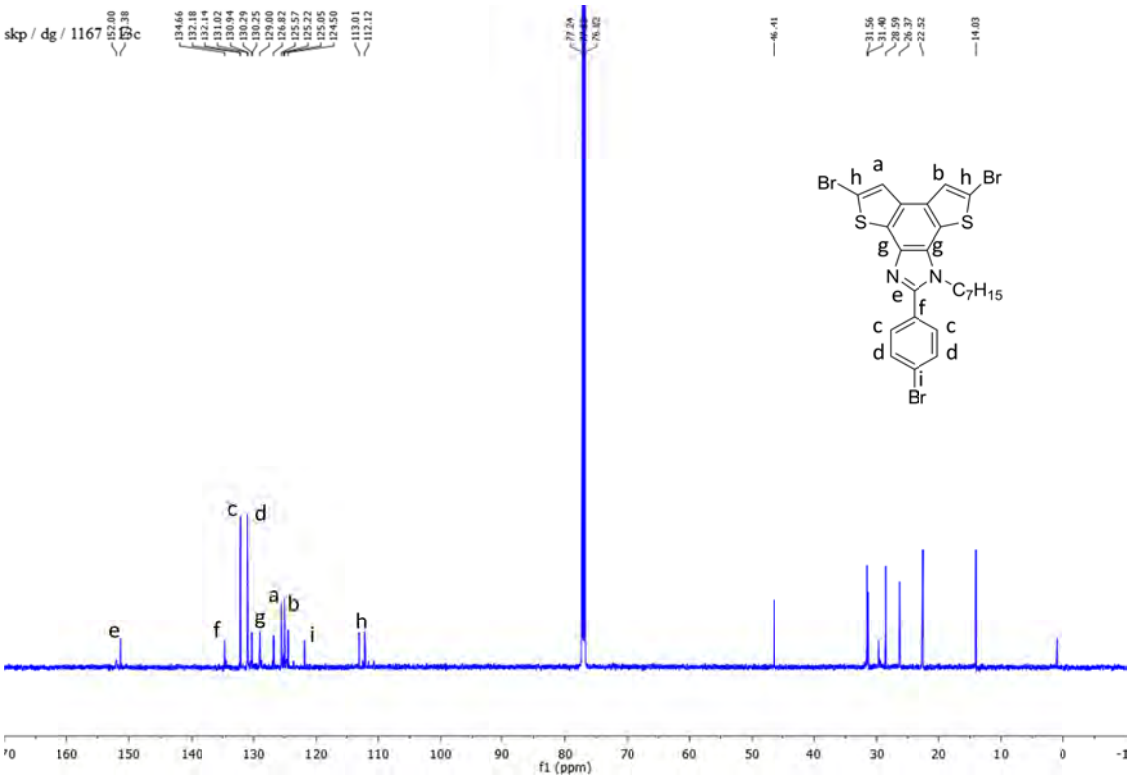

Fig S13: $^{13}C\{^{1}H\}$NMR (150MHz, $CDCl_3$) of **5b**

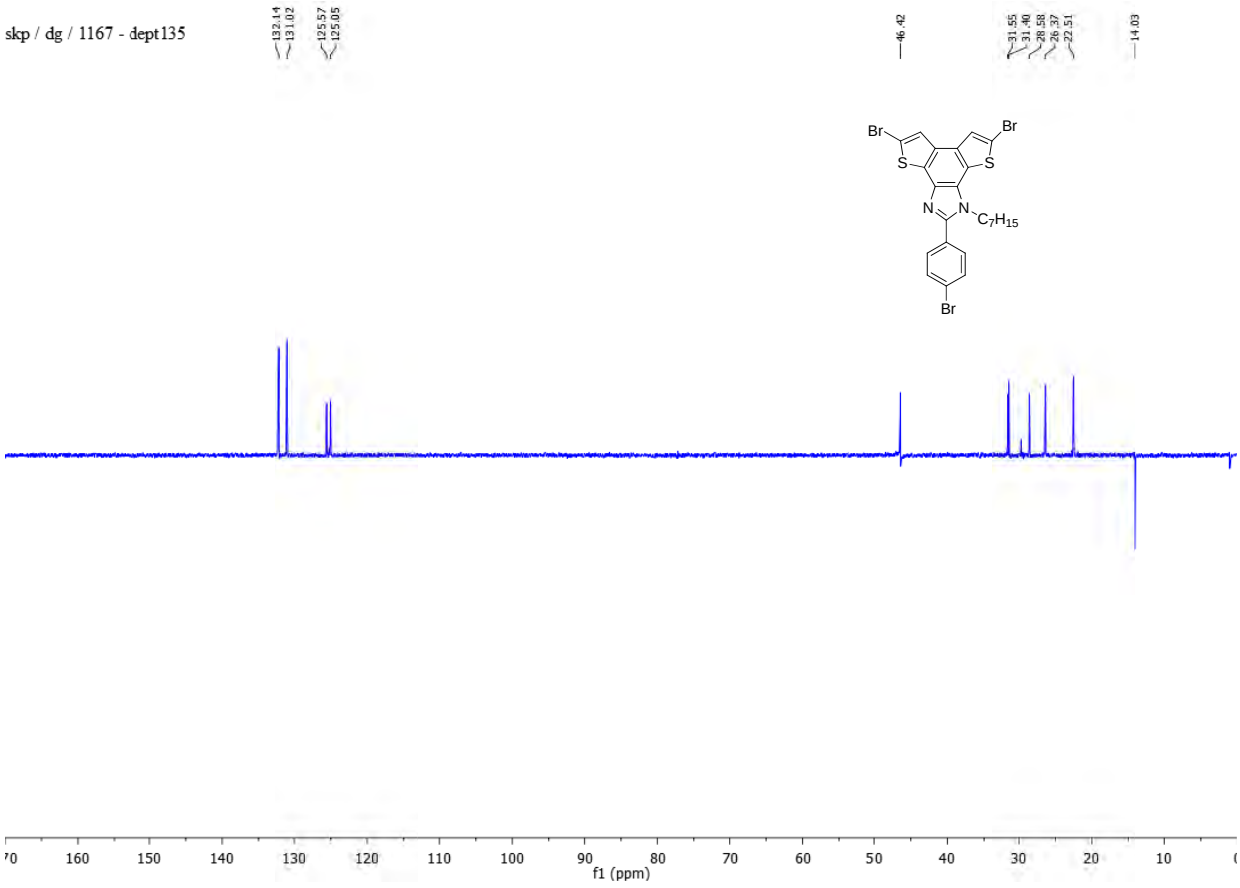

Fig S14: DEPT-135 (150MHz, $CDCl_3$) of **5b**

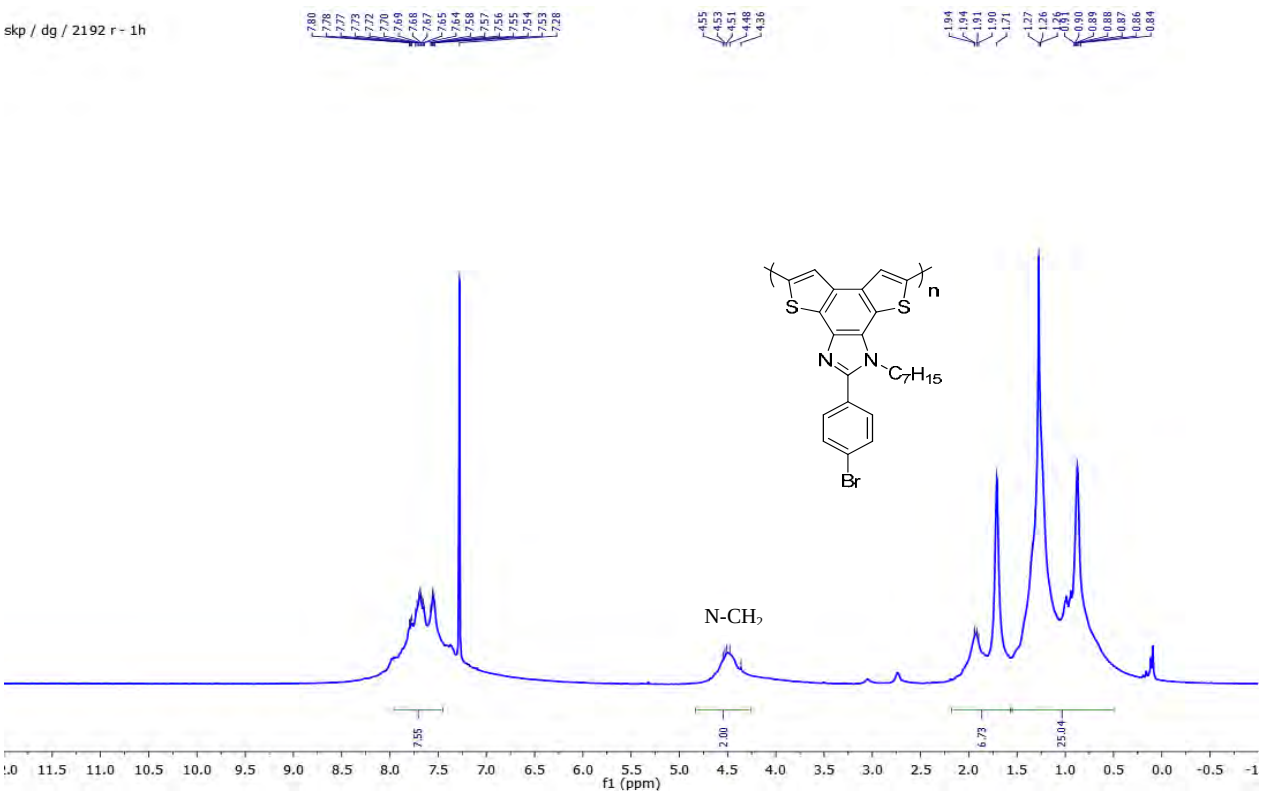

Fig S15: ^{1}HNMR (600MHz, $CDCl_3$) of **P2**

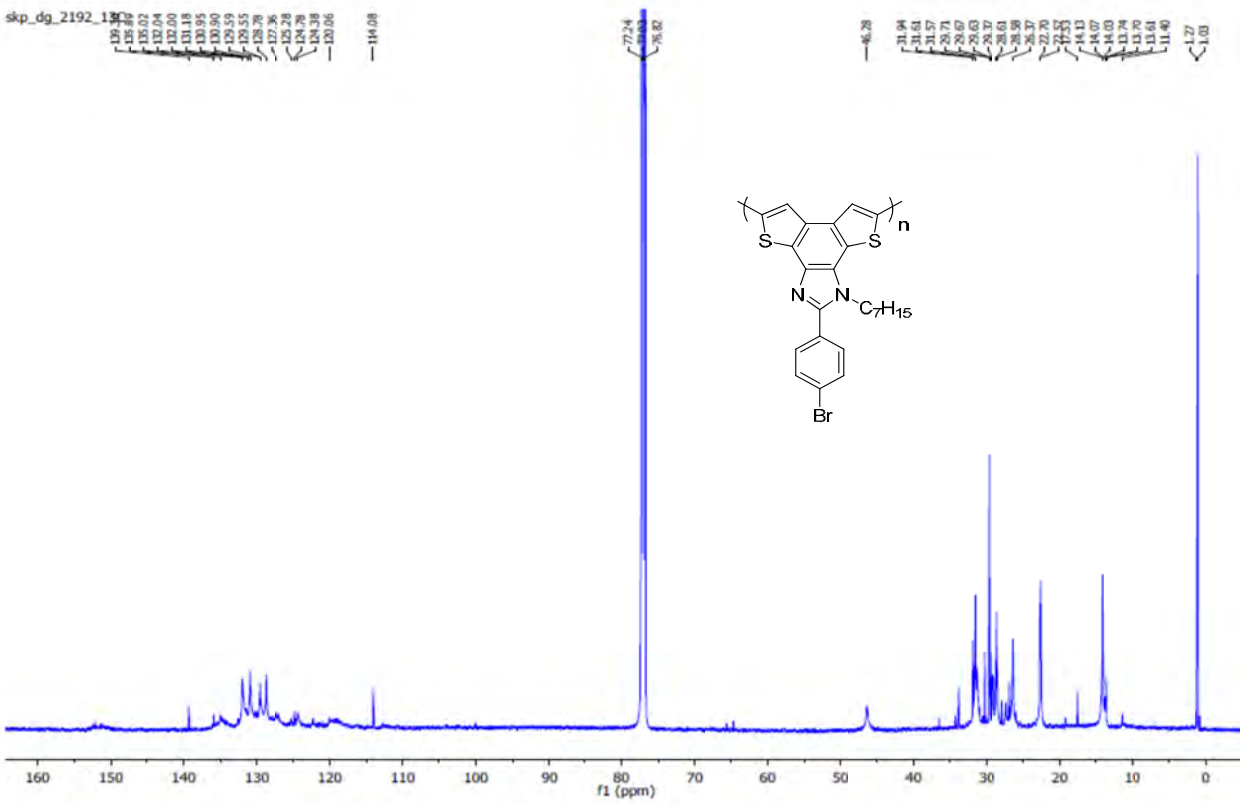

Fig S16: $^{13}C\{^{1}H\}$NMR (150MHz, $CDCl_3$) of **P2**

N-CH_2

Fig S17: ^{1}H NMR (600MHz, $CDCl_3$) of **5a**

Fig S18: $^{13}C\{^{1}H\}$NMR (150MHz, $CDCl_3$) of **5a**

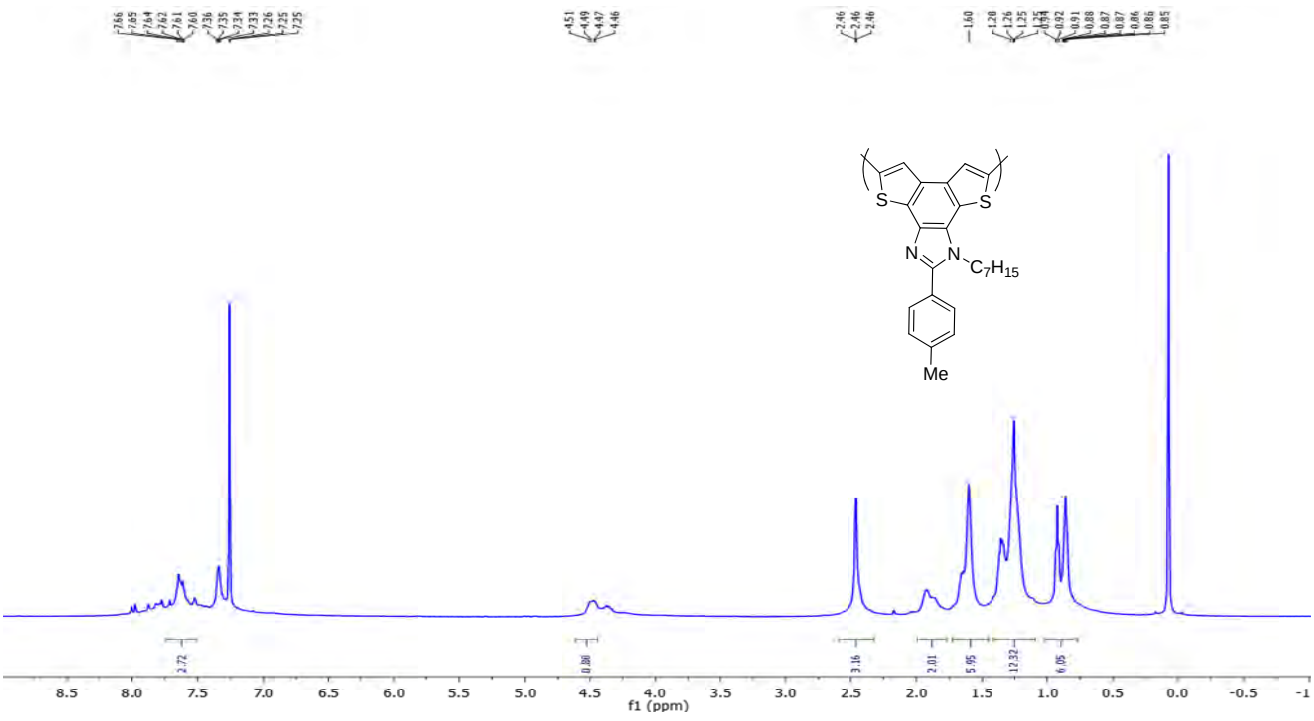

Fig S19: ^{1}H NMR (600MHz, $CDCl_3$) of **P1**

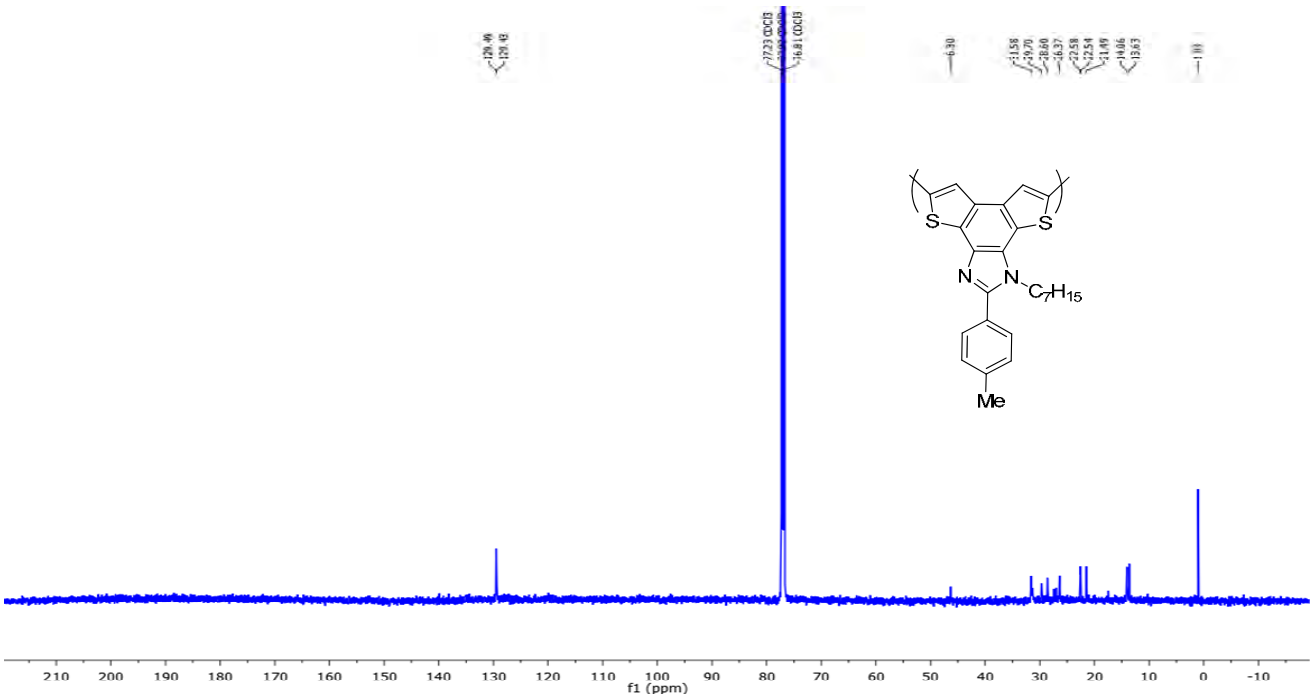

Fig S20: $^{13}C\{^{1}H\}$NMR (150MHz, $CDCl_3$) of **P1**

2b. HRMS data

Fig S21: HRMS(ESI$^+$) spectra of **4a**

Fig S22: HRMS(ESI$^+$) spectra of **4b**

Fig S23: HRMS(ESI^{+}) spectra of **5b**

Fig S24: MALDI-TOF spectra of [(**4b**)$_2$Cu^{2+}] complex

2c. FTIR spectra

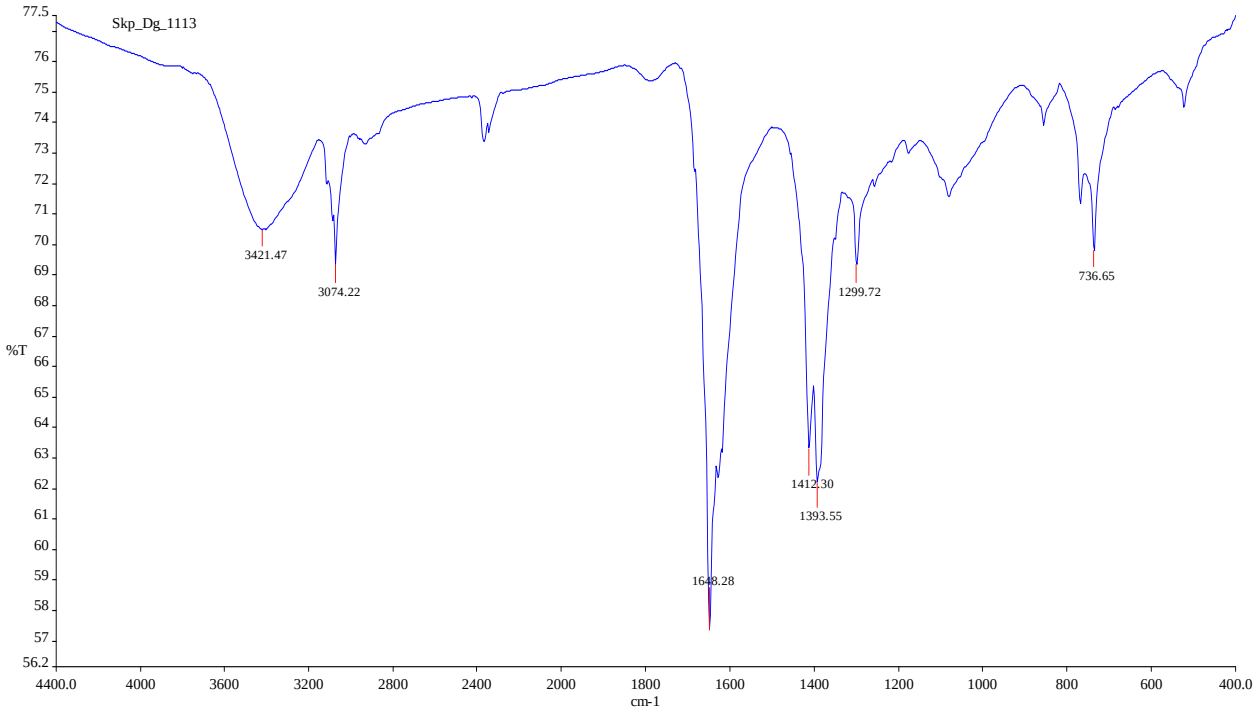

Fig S25: FTIR spectrum of **2**

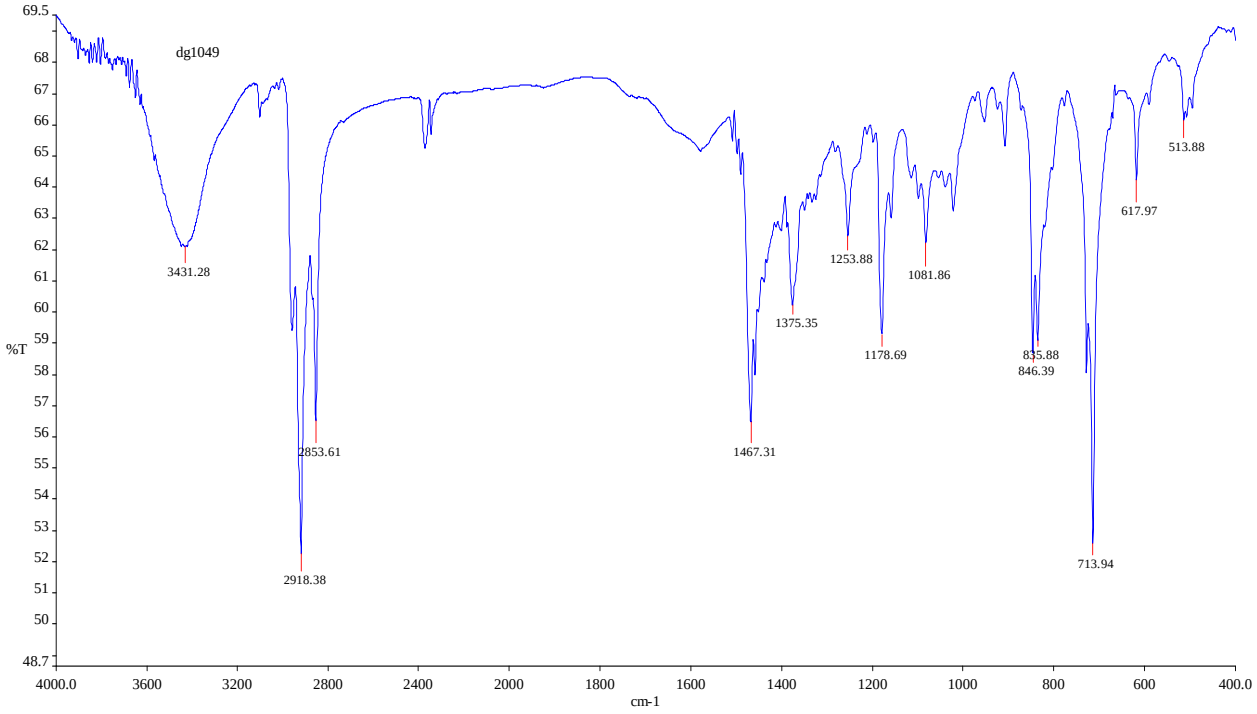

Fig S26: FTIR spectrum of **4a**

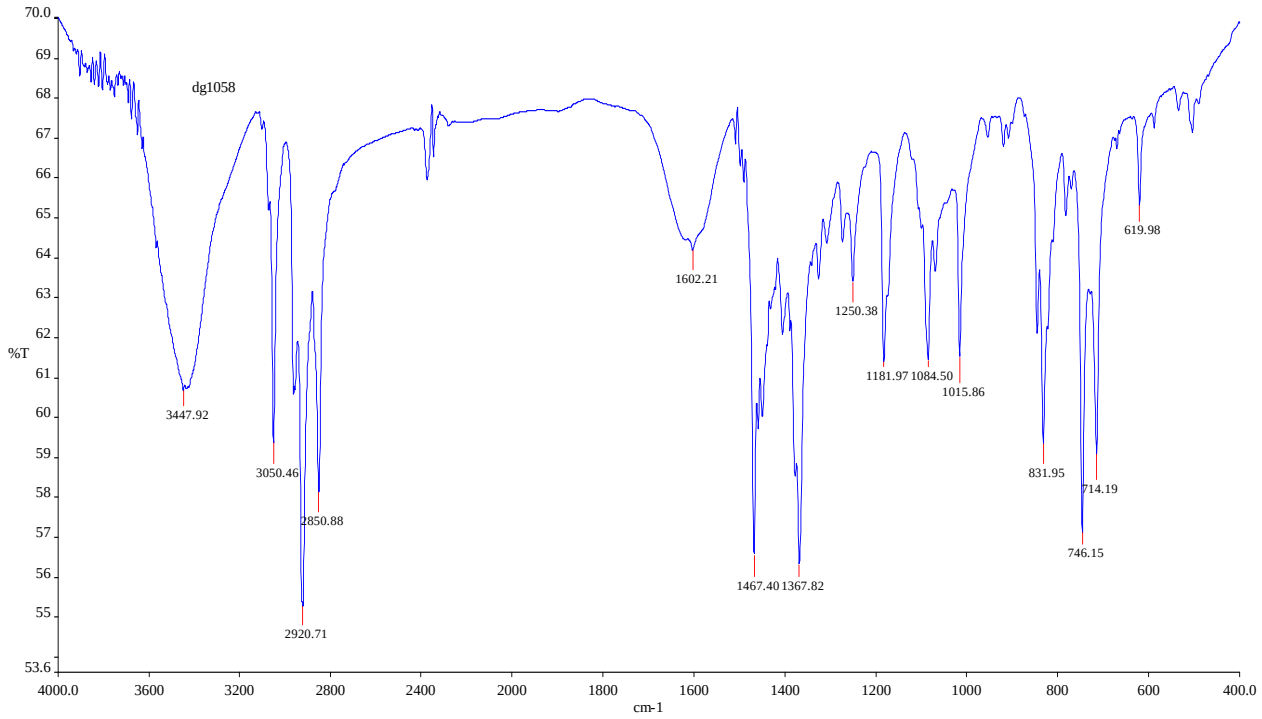

Fig S27: FTIR spectrum of **4b**

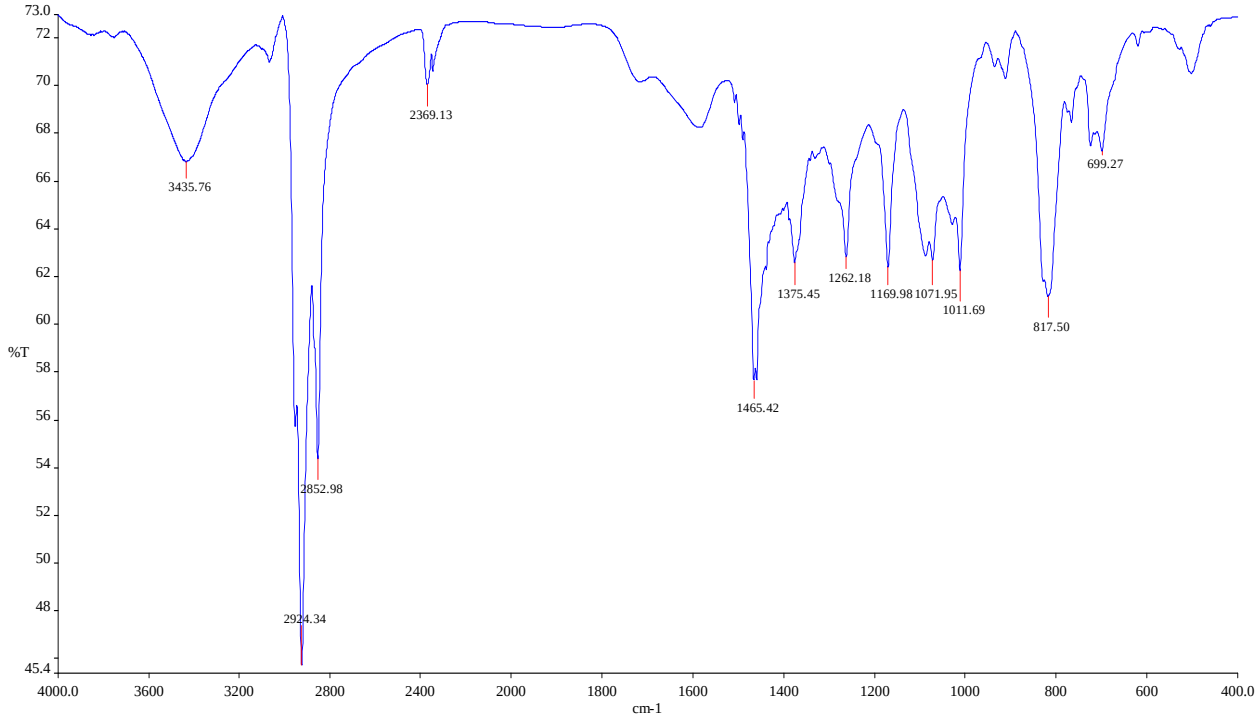

Fig S28: FTIR spectrum of **P2**

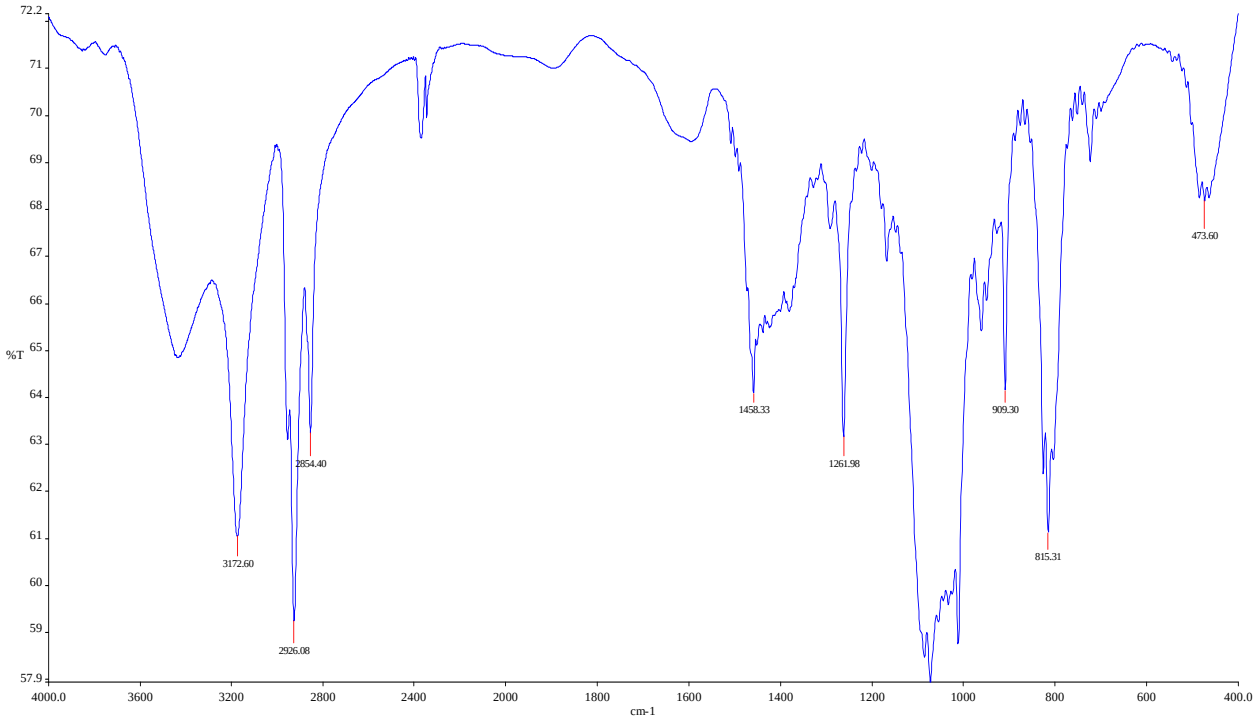

Fig S29: FTIR spectrum of **[(4b)$_2$**·Cu^{2+}]

3. Crystallographic data of 4b

Table S1. Crystallographic Data and Refinement Parameters for **4b.**

	4b
Empirical formula	$C_{24}H_{23}BrN_2S_2$
Formula weight	483.47
Crystal system	Triclinic
Space group	$P\bar{1}$
a, Å	5.3489(14)
b, Å	16.754(4)
c, Å	24.034(6)
α, deg	89.741(8)
β, deg	89.969(9)
γ, deg	89.739(9)
V, $Å^3$	2153.8(10)
Z	4
ρ_{calcd}, g cm^{-3}	1.491
μ, mm^{-1}	21.16
F(000)	992
Reflections	
Collected	27149
independent	8424
observed [I > 2σ(I)]	4551

No. of variables	525
Goodness-of-fit	0.953
Final R indices [$I>2\sigma(I)$][a]	$R_1 = 0.0610$
	$wR_2 = 0.1357$
R indices (all data)[a]	$R_1 = 0.1309$
	$R_1 = 0.1696$

[a]$R_1 = \Sigma||F_o| - |F_c||/\Sigma|F_o|$ with $F_o^2>2\sigma(F_o^2)$. $wR_2 = [\Sigma w(|F_o^2| - |F_c^2|)^2/\Sigma|F_o^2|^2]$

4a. Attempted GRIM polymerization

Table S2: Attempted GRIM polymerization of **5a** and **5b.**

Sl. No	Reagent	Solvent	Time (hours)	Polymer
1	t-BuMgCl, Ni(dppp)Cl_2, 60^{o}C	THF	48	No
2	i-PrMgBr, Ni(dppp)Cl_2, 60^{o}C	THF	60	No
3	i-PrMgBr, Ni(dppp)Cl_2, LiCl 60^{o}C	THF	48	No
4	CyclohexylMgBr, Ni(dppp)Cl_2, 60^{o}C	THF	50	No

4b. Tetradetector GPC studies of P1 and P2

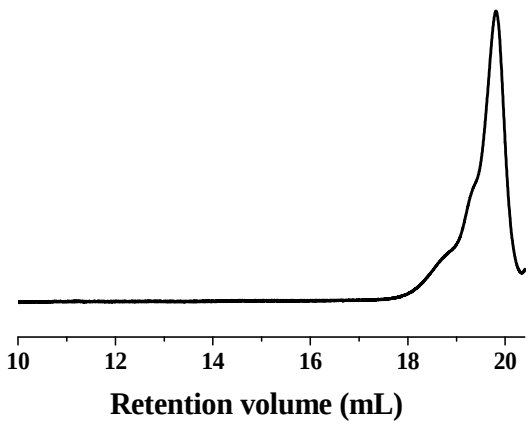

Fig S30: GPC trace, Refractive Index response of **P2.** PDI (M_w/M_n) of **P2** was found to be 1.67.

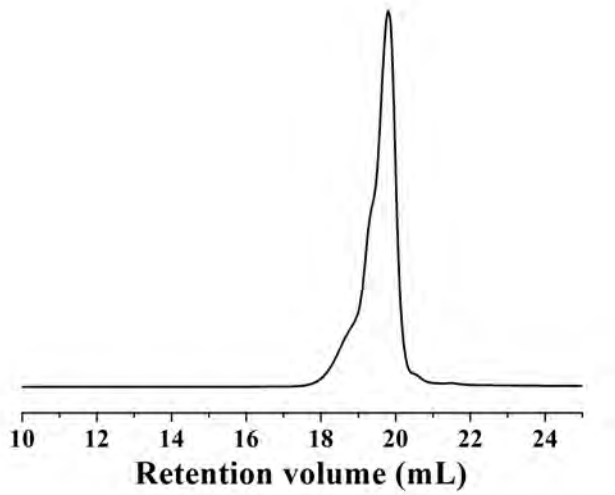

Fig S31: GPC trace, UV response of **P2** using THF as eluent.

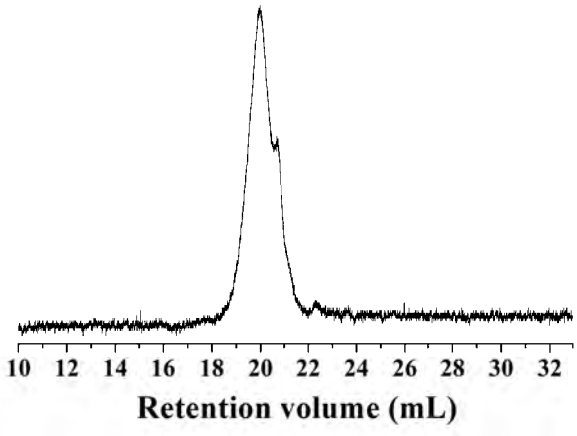

Fig S32: GPC trace, RALS response of **P2** using THF as eluent**.**

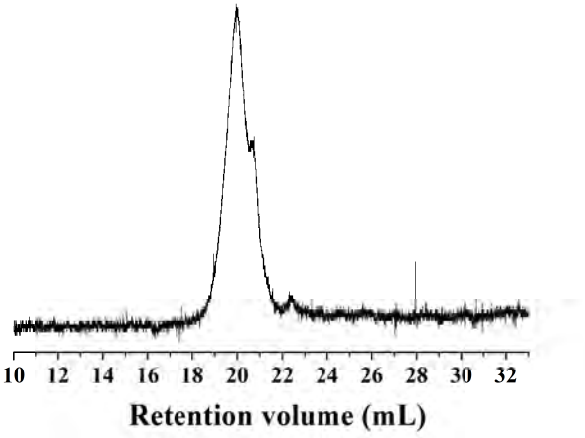

Fig S33: GPC trace, LALS response of polymer **P2** using THF as eluent.

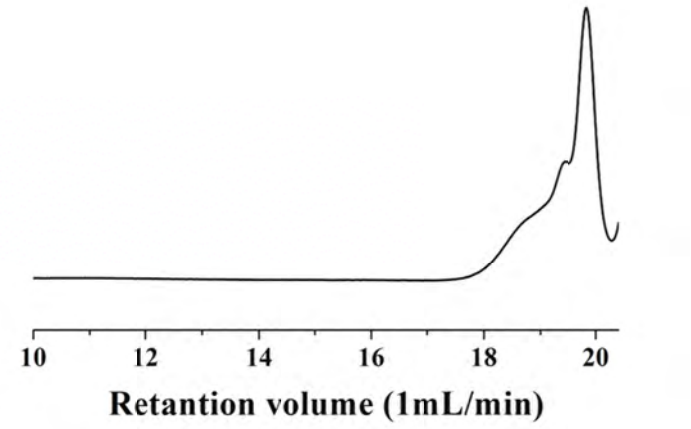

Fig S34: GPC trace, Refractive Index response of **P1.** PDI (M_w/M_n) of **P1** was found to be 1.81.

5a. Photophysical properties of 4a and 4b

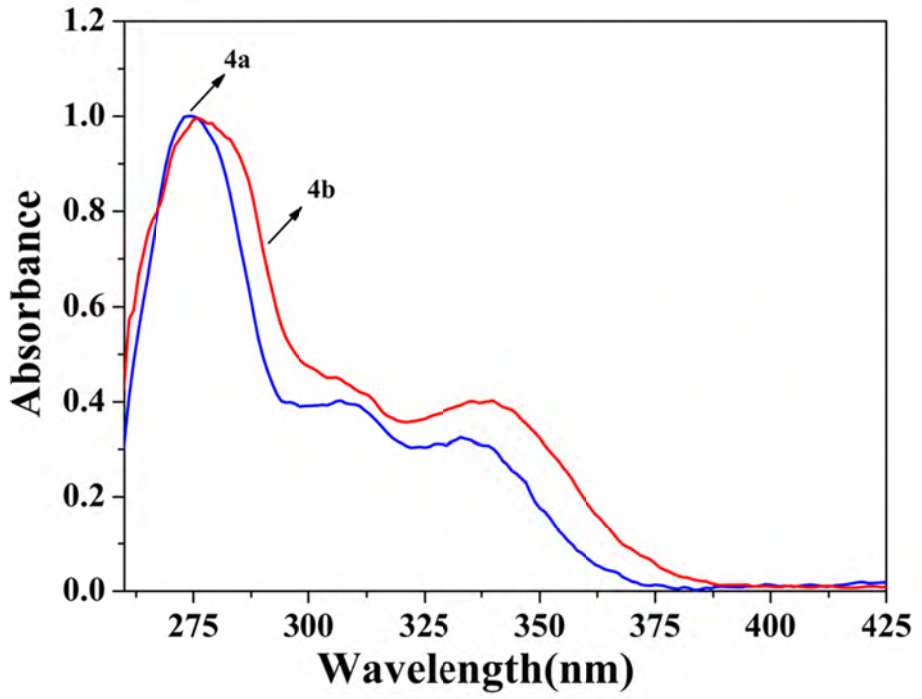

Fig S35: Absorbance spectra of **4a** and **4b** in DMSO:H_2O(1:1) in~2 x 10^{-5}M

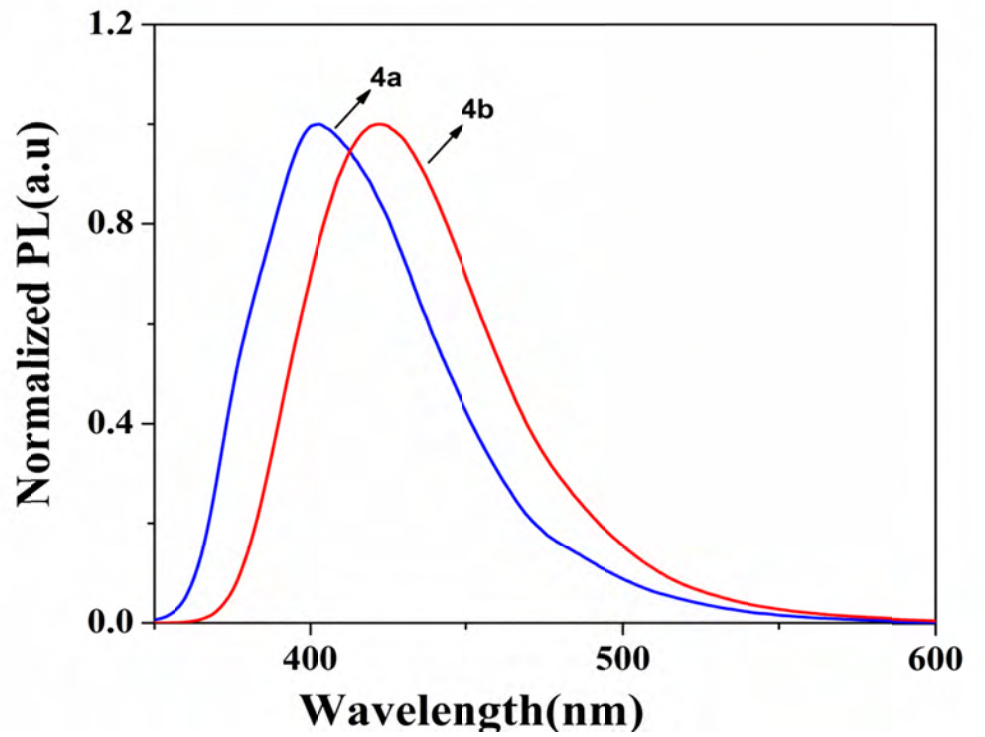

Fig S36: Emission spectra of **4a** and **4b** in DMSO:H_2O(1:1) excited at 333 nm and 340 nm respectively.

5b. Photophysical response of 4a with various metal ion

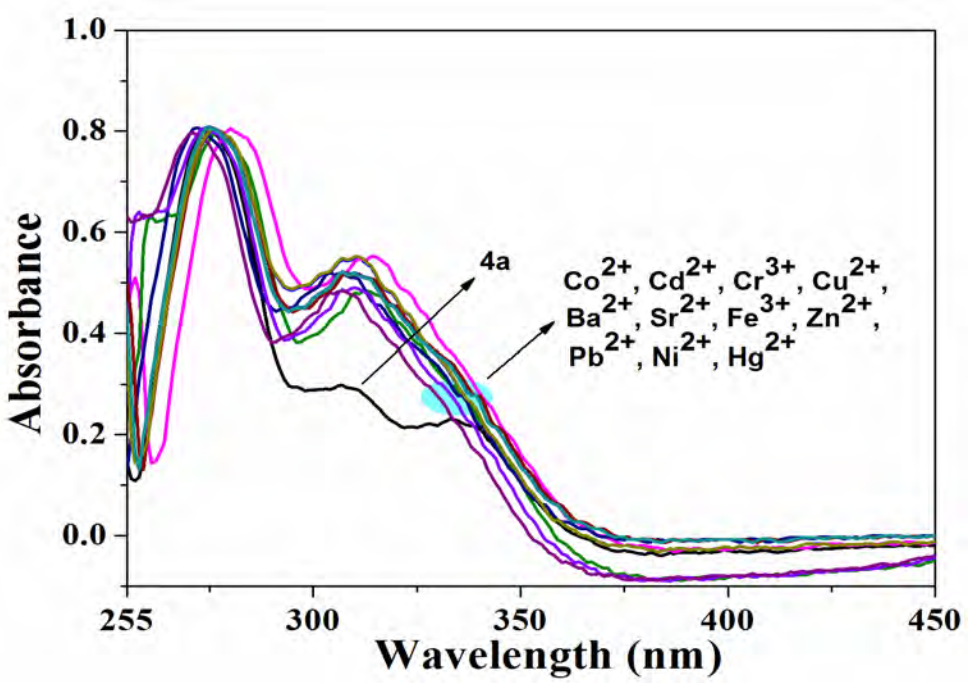

Fig S37: Absorbance spectra of **4a** (~2 x 10^{-5} M) in presence of different metal ion in DMSO:H_2O (1:1)

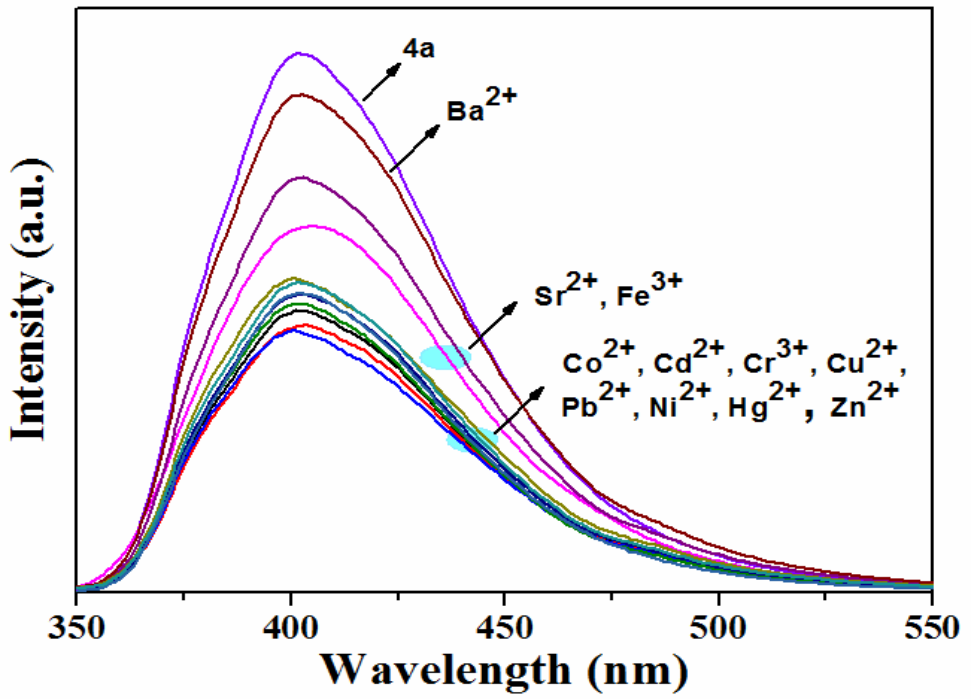

Fig S38: Emission spectra of **4a** (~2 x 10^{-5} M) in presence of different metal ion in DMSO:H_2O (1:1) excited at 333 nm.

5c. Selective Cu^{2+} reorganization studies by 4b

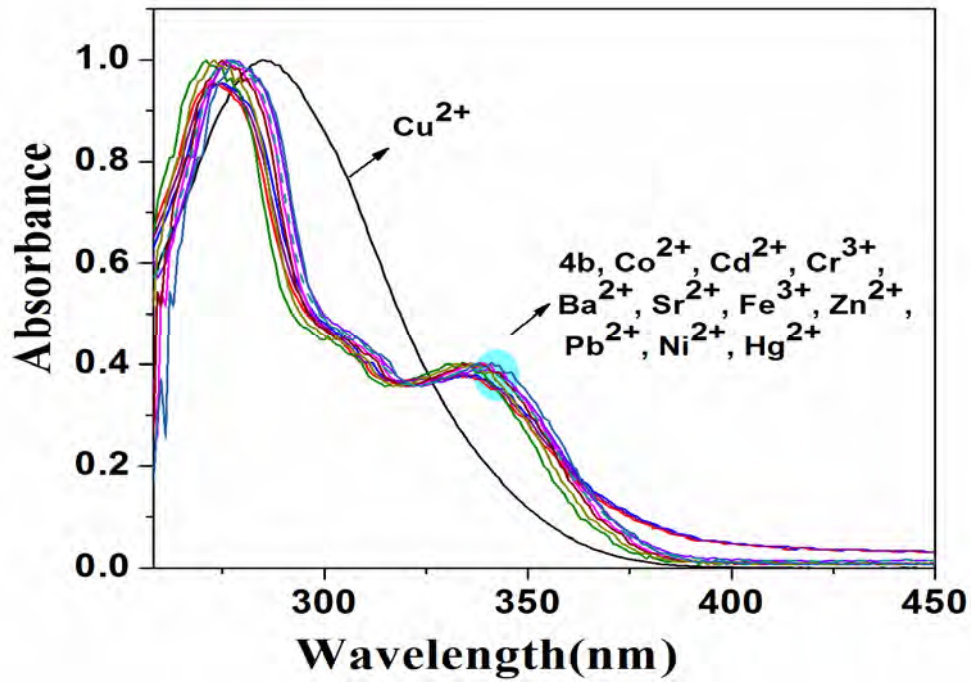

Fig S39: Absorption spectra of **4b** (~2 x 10^{-5} M) in presence of different metal ion in DMSO:H_2O (1:1).

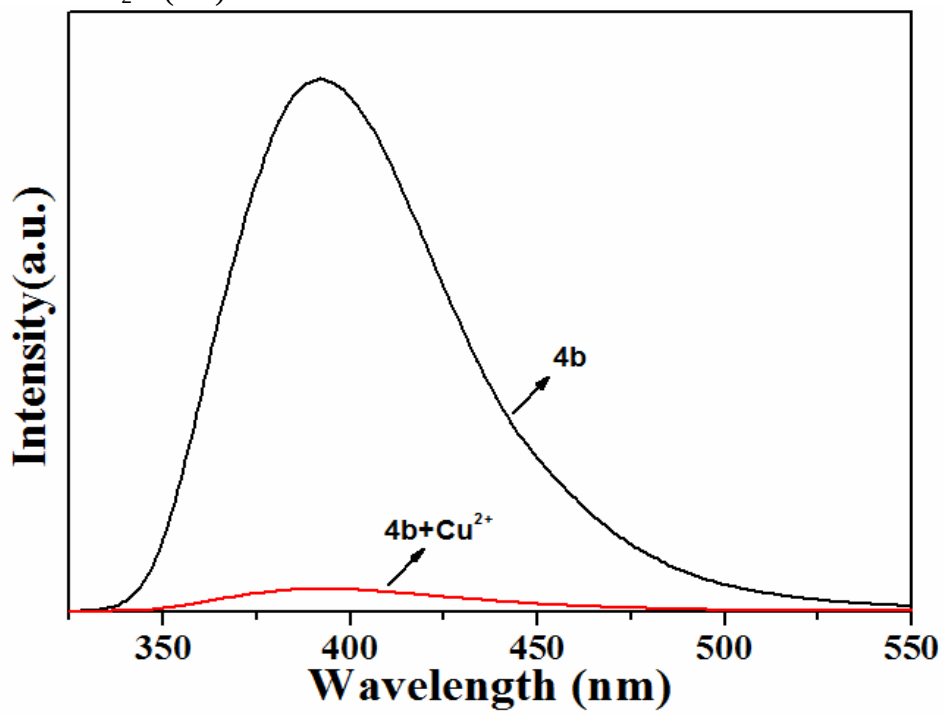

Fig S40: Emission spectra of **4b** (~2 x 10^{-5} M) and **4b** in presence of Cu^{2+} metal ion in DMSO:H_2O (1:1) excited at 340 nm.

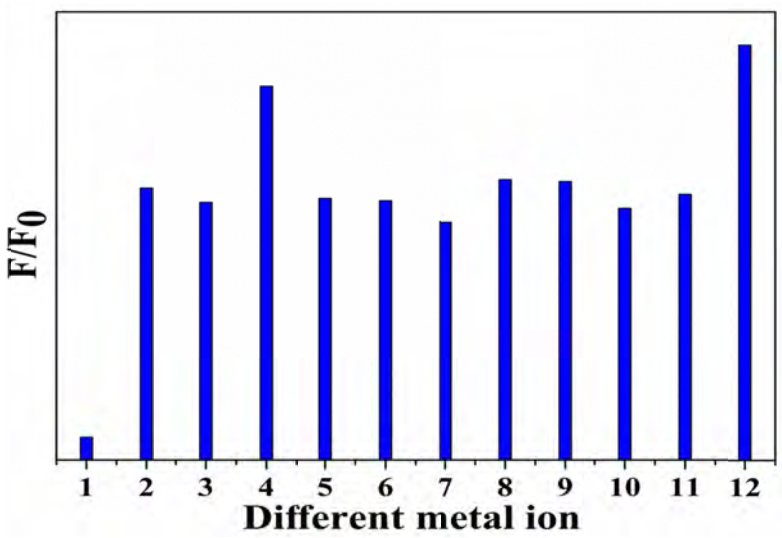

Fig S41: Selectivity sensing of **4b** in presence of different metal ion. 1-12 represent (1) **4b**+Cu^{2+}; (2) **4b** + Cd^{2+}; (3) **4b** + Sr^{2+}; (4) **4b** + Ba^{2+}; (5) **4b** + Co^{2+}; (6) **4b** + Fe^{3+}; (7) **4b** + Zn^{2+}; (8) **4b** + Cr^{3+}; (9) **4b** + Ni^{2+}; (10) **4b** + Pb^{2+}; (11) **4b** + Hg^{2+}; (12) **4b**.

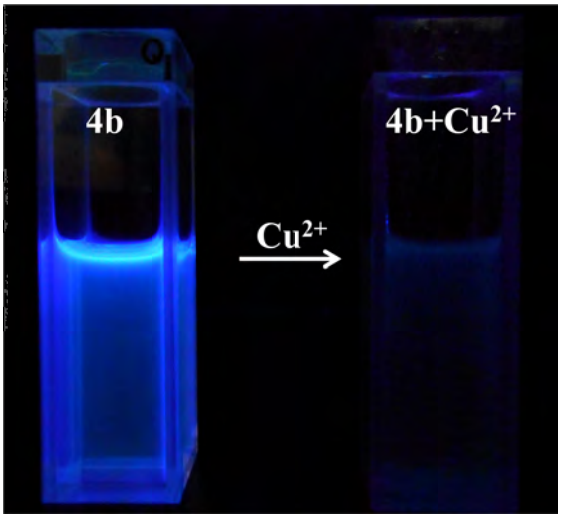

Fig S42: Photograph of **4b** and **4b** in presence of Cu^{2+} metal ion in DMSO:H_2O (1:1) under the illumination of 365 nm light.

5d. Titration studies by continuous variation of Cu^{2+} ion concentration

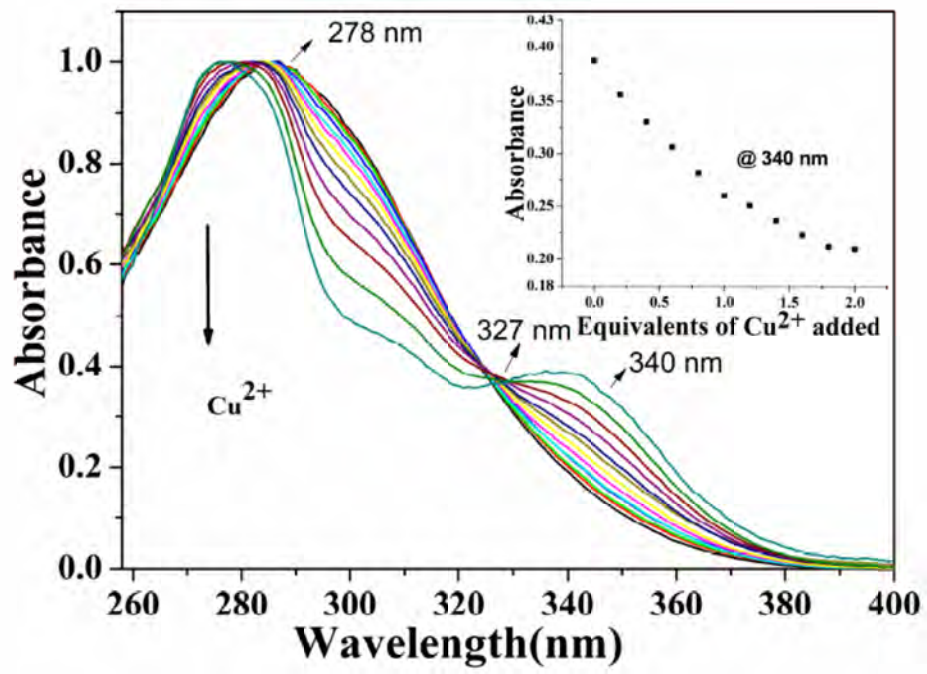

Fig S43: Absorbance spectra change of **4b** (~ 2x 10^{-5}) in DMSO:H_2O (1:1) with increasing equivalent of Cu^{2+}.

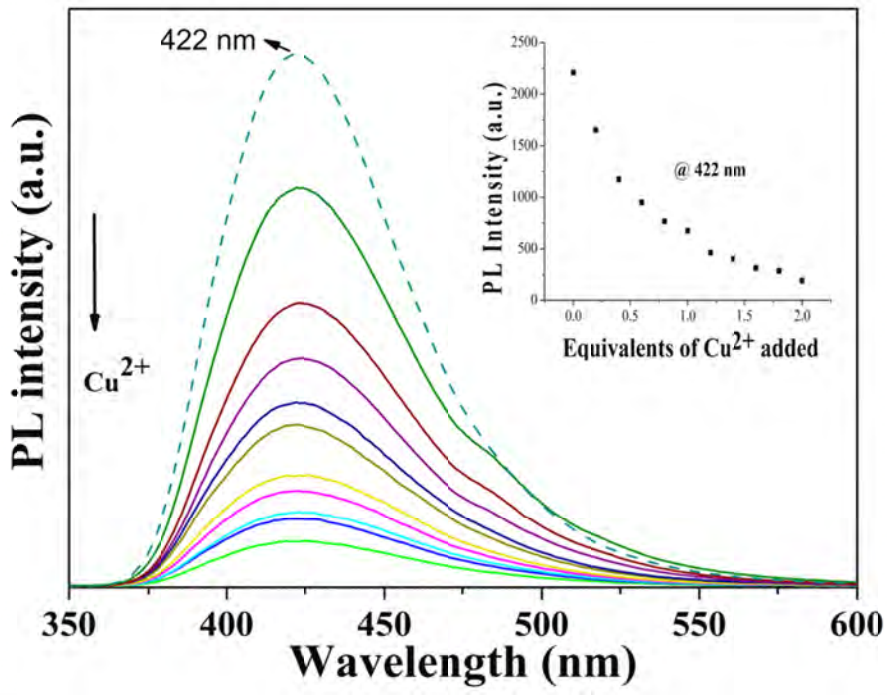

Fig S44: Emission spectral response of **4b** (~ 2x 10^{-5}) in DMSO:H_2O (1:1) with increasing equivalent of Cu^{2+}.

5e. Stern-Volmer plot

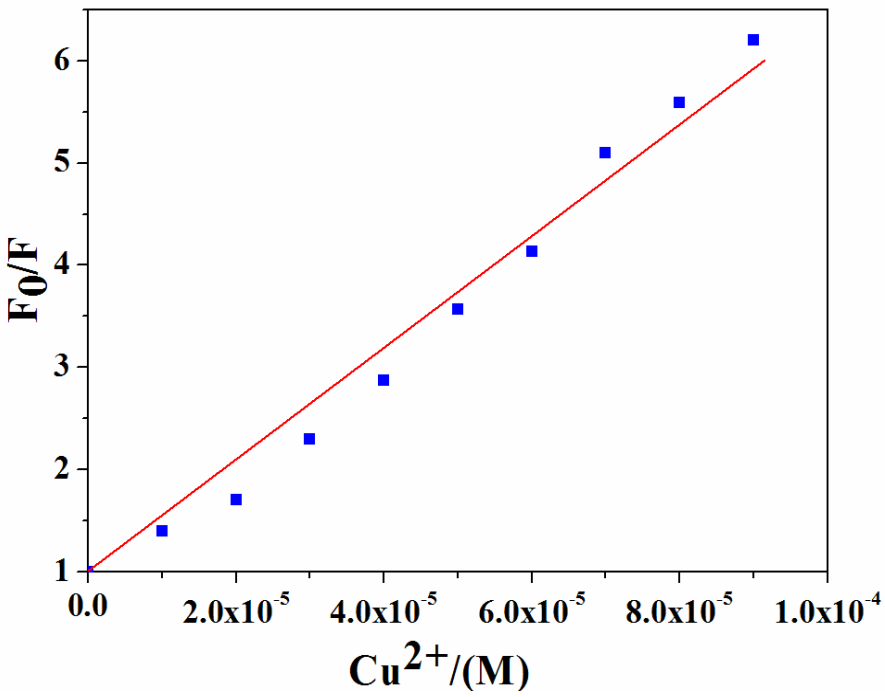

Fig S45: Stern-Volmer plot of **4b** and Cu^{2+} association. Where F_0 is the fluorescence intensity in the absence of added quencher, Fis the fluorescence intensity as a function of quencher concentration [Q]. The slope of the plots F_0/F vs [Q] gives the Stern-Volmer quenching constant (K_{SV}) and linear relationship of [Q] with F_0/F implies the purely static quenching.

5f. Photophysical properties of P1 and P2

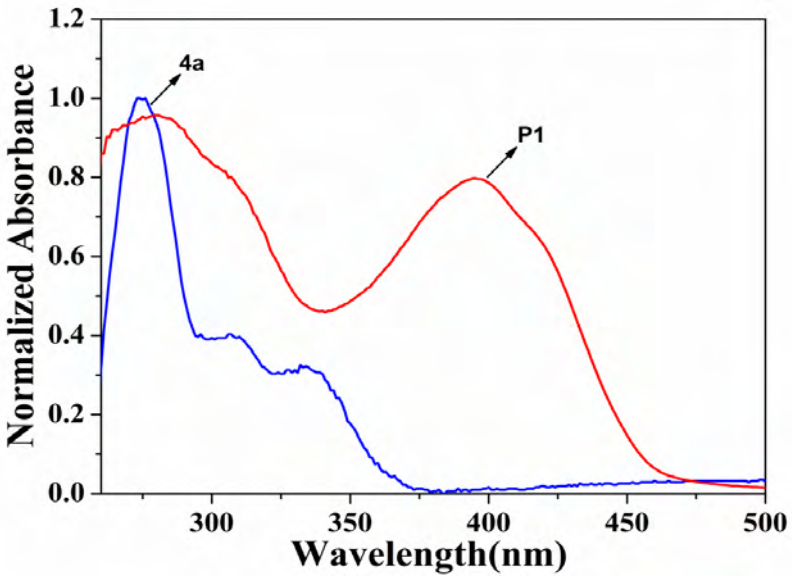

Fig S46: Absorbance spectra of **4a** and **P1** in DMSO:H_2O(1:1) in~2 x 10^{-5}M.

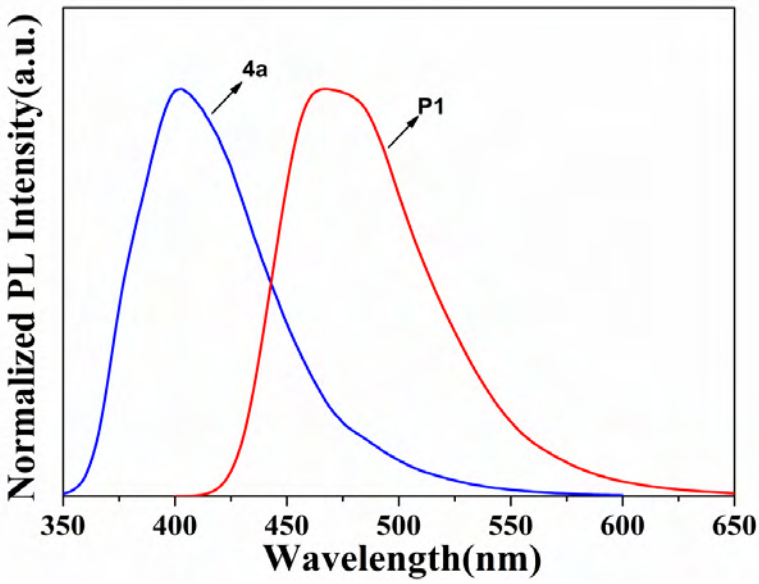

Fig S47: Emission spectra of **4a** and **P1** in DMSO:H_2O(1:1) excited at 333 nm and 395 nm respectively.

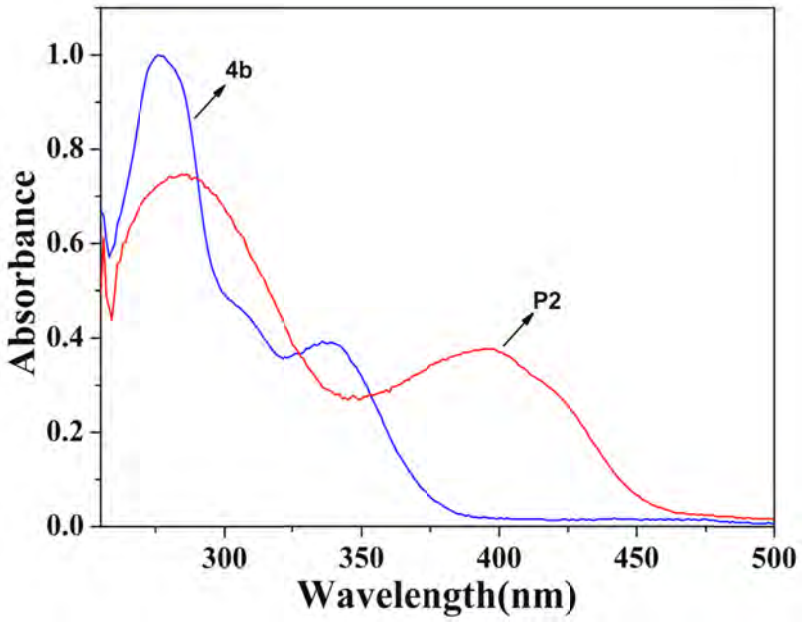

FigS48: Absorbance spectra of **4b** and **P2** in DMSO:H_2O(1:1) in~2 x 10^{-5}M.

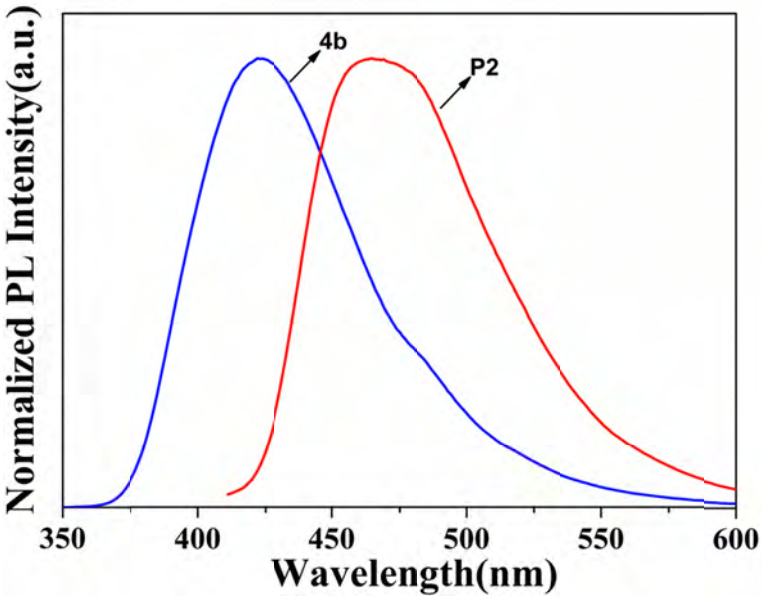

Fig S49: Emission spectra of **4b** and **P2 i**n DMSO:H_2O(1:1) excited at 340 nm and 400 nm respectively.

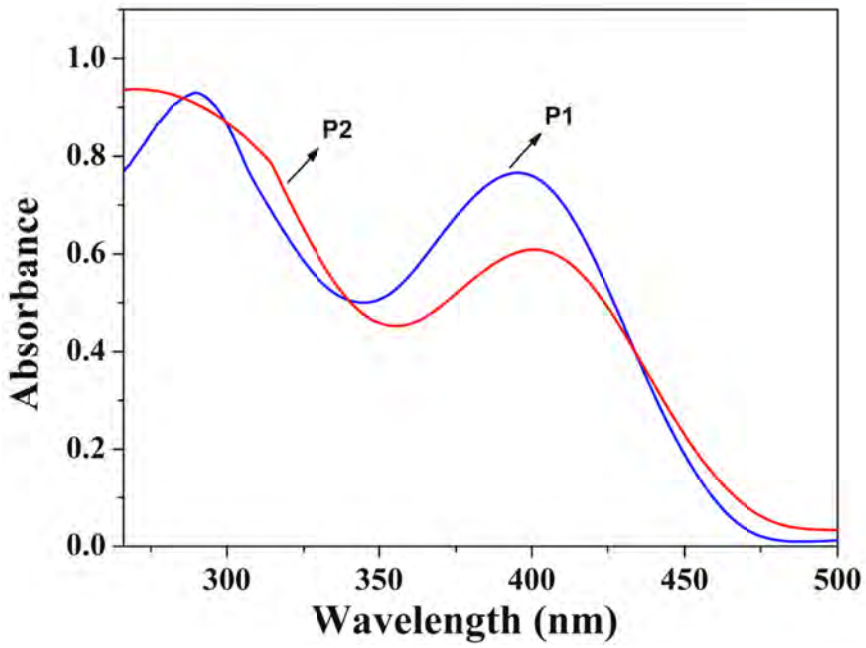

Fig S50: Absorbance spectra of **P1** and **P2** in DMSO:H_2O(1:1).

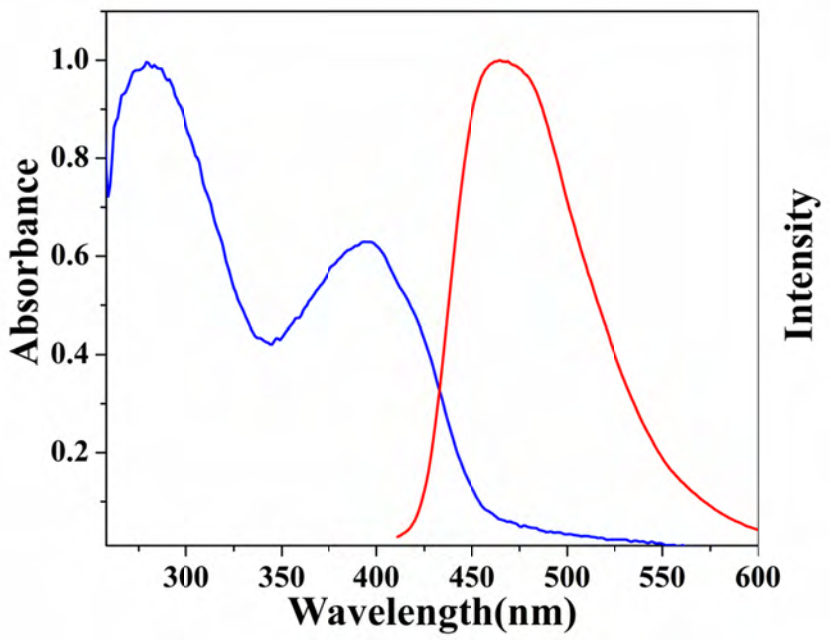

Fig S51: Absorbance and emission spectra of **P2** in DMSO:H_2O(1:1) in~2 x 10^{-5} M.

5g. Determination of Limit of Detection (LOD)

The limit of detection (LOD) was calculated from the following equation.[4]

LOD = 3σ/s, where 'σ' is the standard deviation of blank measurements, and 's' is the slope between fluorescence intensity and Cu^{2+} concentration.

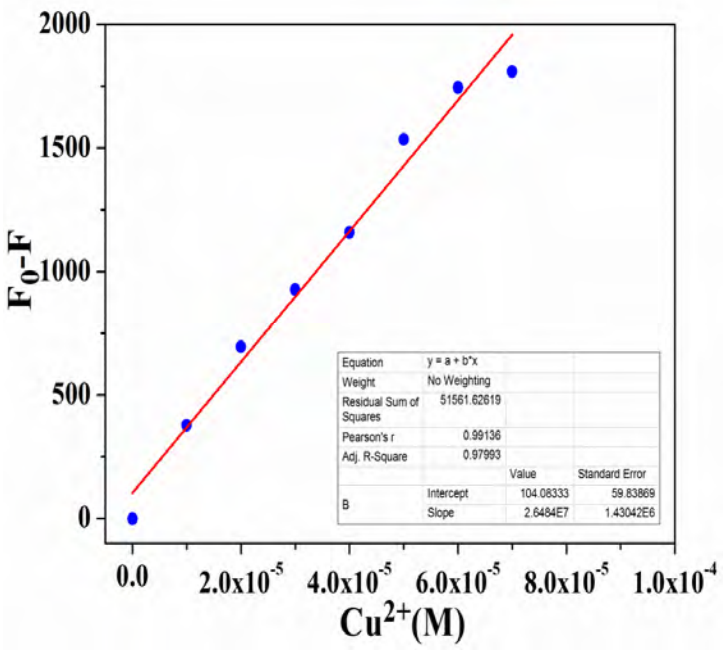

Fig S52a: Changes of Fluorescence Intensity of **4b** (2 x 10^{-5} M in 1:1 DMSO-H_2O) as a function of [Cu^{2+}] at 422 nm.

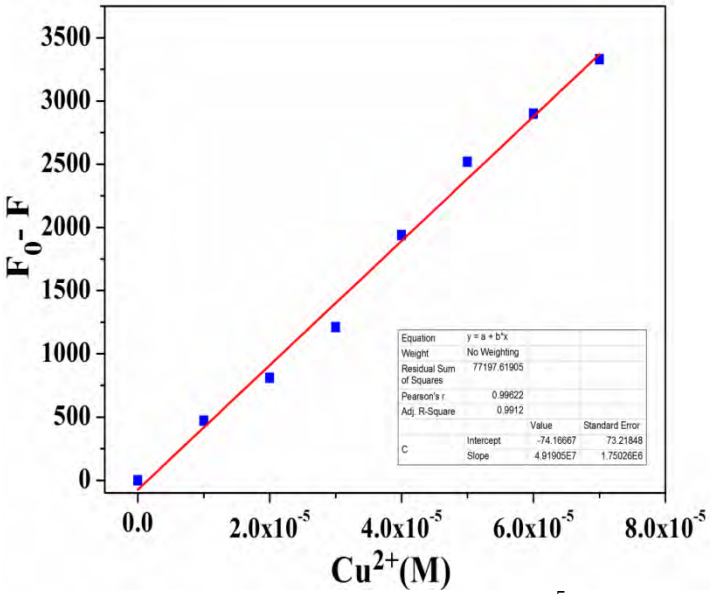

Fig S52b: Changes of Fluorescence Intensity of **P2** (2 x 10^{-5} M in 1:1 DMSO-H_2O) as a function of [Cu^{2+}] at 468 nm.

5h. Calculation of HOMO and LUMOs of the fluorophores by electrochemical studies and proposed mechanism of PL quenching through electron transfer.

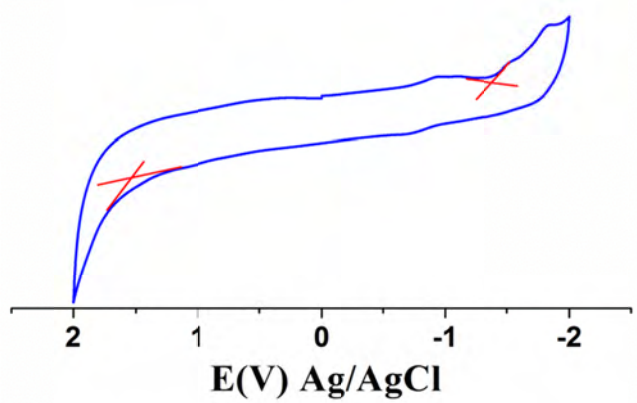

Fig S53a: Cyclic voltammogram of **4a**, film casted on GC disc working electrode using $TBAPF_6$ as supporting electrolyte in MeCN, Ag/AgCl as reference electrode and Pt wire as auxiliary electrode. Scan rate at 100 mV/s.

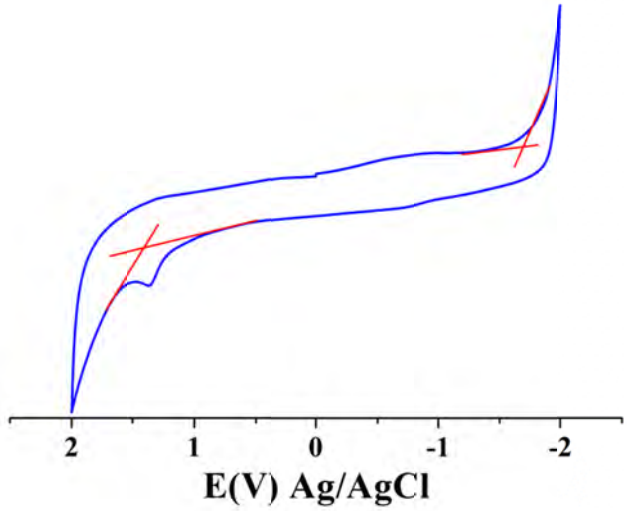

Fig S53b: Cyclic voltammogram of **4b**, film casted on GC disc working electrode using $TBAPF_6$ as supporting electrolyte in MeCN, Ag/AgCl as reference electrode and Pt wire as auxiliary electrode. Scan rate at 100 mV/s.

Determination of HOMO and LUMO from CV studies: The HOMO and LUMO energy levels for **4a** and **4b** in solid state were estimated by conventional electrochemical techniques. The solution of **4a** and **4b** were drop casted onto the glossy carbon disc electrode from their DCM solutions. Cyclic voltammetry of films of **4a** and **4b** (prepared by drop casting) were performed in CH_3CN using *n*-Bu_4NPF_6 as the supporting electrolyte. Ag/AgCl and Pt wire were used as reference and auxiliary electrodes respectively. The HOMO energy level (E_{HOMO}) was calculated from the onset oxidation potential (E_{onset}) using the following equation: $E_{HOMO} = -(E_{onset}^{ox} + 4.4)$ eV, and the LUMO energy level (E_{LUMO}) was calculated from the onset reduction potential (E_{onset}) using the following equation: $E_{LUMO} = -(E_{onset}^{red} + 4.4)$ eV, where the energy level was calibrated against the Ag/AgCl couple.

Fluorophore	E_{HOMO}(eV)[a]	E_{LUMO}(eV)[b]	E_g(eV)
4a	-5.93	-3.02	2.91
4b	-5.79	-2.71	3.08

Fig S54a: Electron transfer mechanism involving the excited **4b** and d^9 Cu^{2+} ion in an elongated octahedral coordination environment (having the unpaired electron in $d_{x^2-y^2}$ orbital) leading to PL quenching.

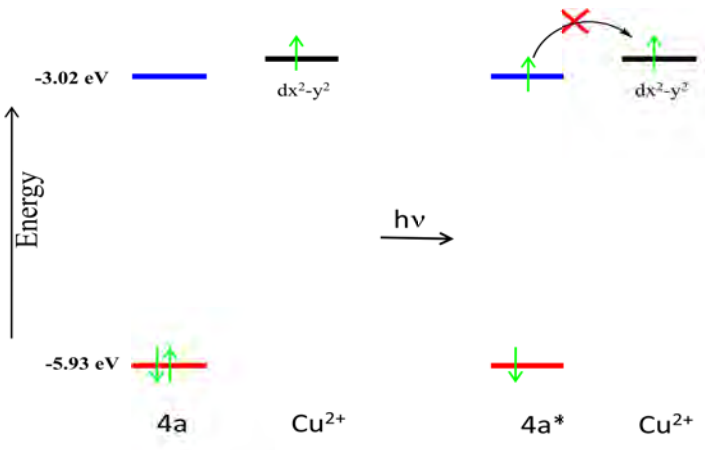

Fig S54b: Demonstration of the unsuccessful electron transfer involving the excited **4a** and d^9 Cu^{2+} ion in an elongated octahedral coordination environment (having the unpaired electron in $d_{x^2-y^2}$ orbital) leading no change in PL intensity.

5i. Electrochemical characterization **4b.Cu^{2+}** and **P2.Cu^{2+}**

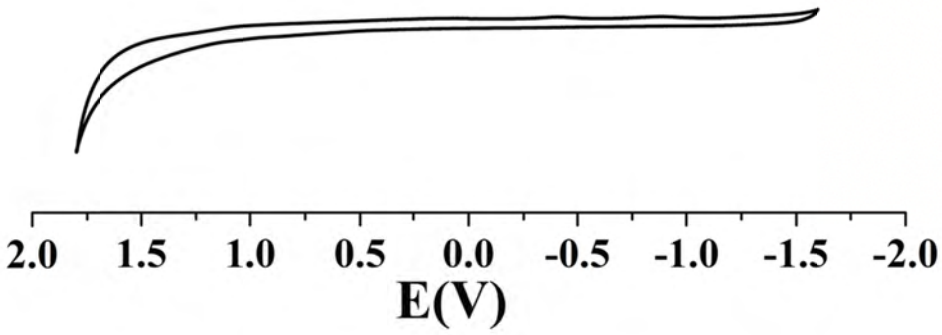

Fig S55a: Cyclic voltammogram of DMF using [(*n*-Bu)$_4$N]PF$_6$ as supporting electrolyte (Blank run), Pt disc working electrode, Pt wire auxiliary electrode and Ag/AgCl reference electrode. Scan rate at 100mV/s.

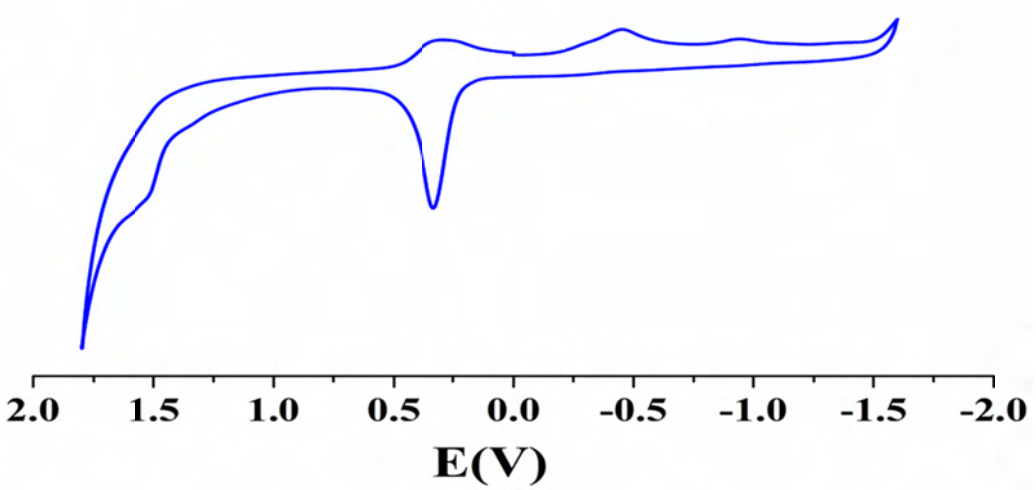

Fig S55b: Cyclic voltammogram of **4b.Cu^{2+}** in DMF using [(*n*-Bu)$_4$N]PF$_6$ as supporting electrolyte, Pt disc working electrode, Pt wire auxiliary electrode and Ag/AgCl reference electrode. Scan rate at 100mV/s.

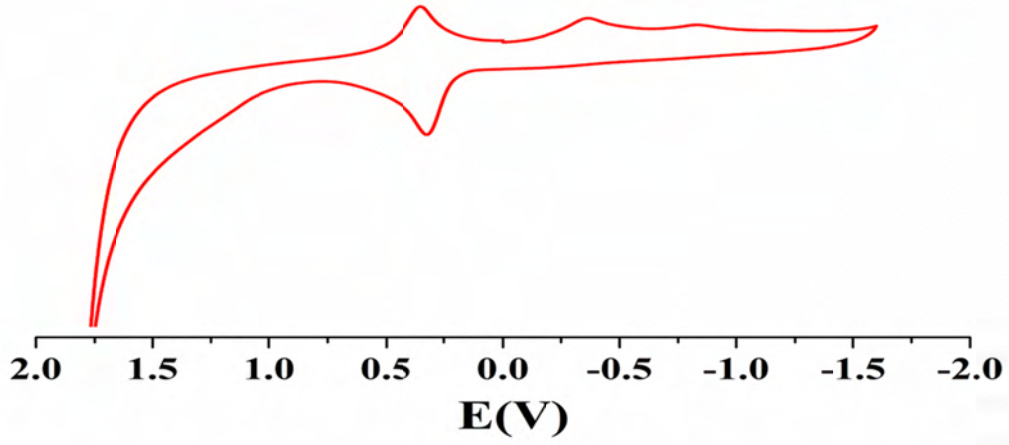

Fig S55c: Cyclic voltammogram of **P2.Cu^{2+}** in DMF using TBA**P**F$_6$ as supporting electrolyte, Pt disc working electrode, Pt wire auxiliary electrode and Ag/AgCl reference electrode. Scan rate at 100mV/s.

5j. Cu^{2+} sensing by thin film of P2 with time

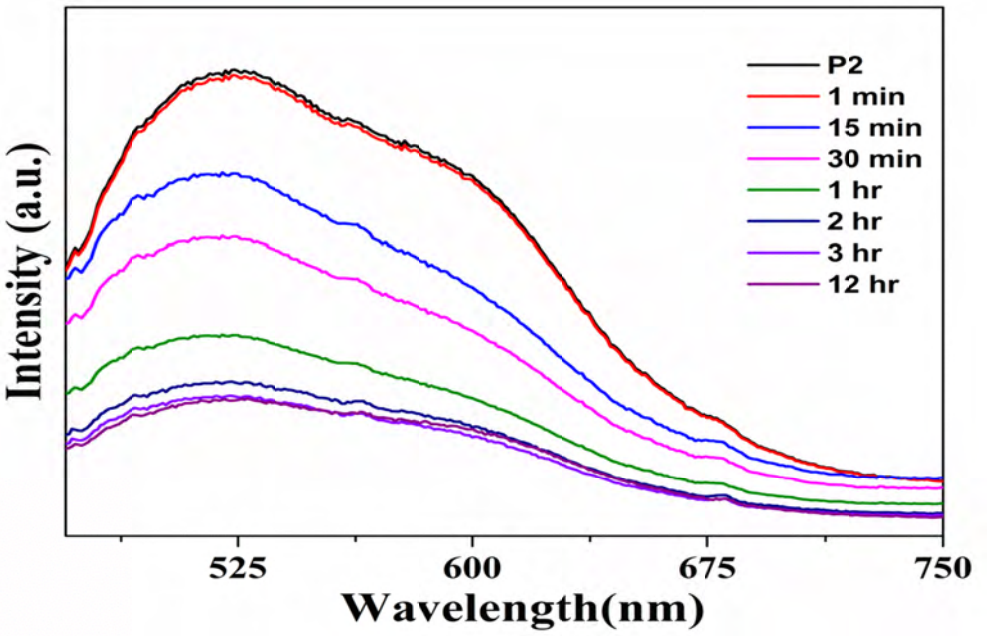

Fig S56: Solid state PL spectra of **P2** thin film (on quartz plate) dipped in Cu^{2+} solution with increasing dipping time.

5k. SEM and EDX analysis of P2 and P2.Cu^{2+}

Preparation of sample for SEM and EDX analysis:

After cleaning the quartz substrate (described previously in page 2, SI), thin film of the polymer **P2**was prepared by spin coating on a 1.7 cm x 1.5 cm quartz plate. A solution of **P2** in toluene (~ 5 x 10^{-4}M) was dropped on the quartz plate and it was spin coated at 5000 rpm for 60 second followed by 8000 rpm for 120 seconds. The surface morphology (by SEM) and EDX analysis were performed. The same polymer film was dipped in aqueous Cu^{2+} solution for 30 min followed by repetitive and extensive washing(at least 20 times) by Milli-Q water to remove any unbound (free) Cu^{2+} ion. The surface morphology and EDX analysis were analyzed. Formation of Cu^{2+}coordinated metallopolymer (**P2**.Cu^{2+}) was confirmed by EDX analysis. Silicone is from the quartz substrate.

a b

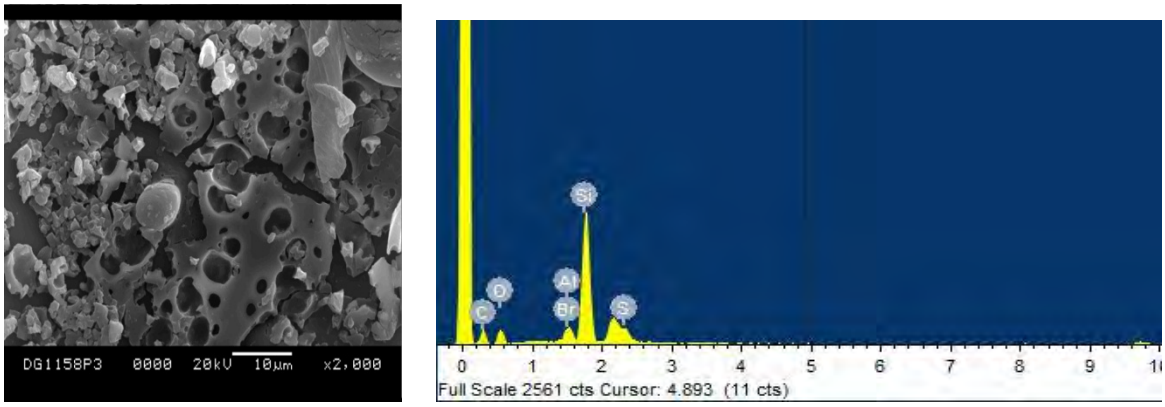

Fig S57: a) SEM image of Polymer **P2** film on quartz plate, b) EDX analysis of polymer **P2.**

a b

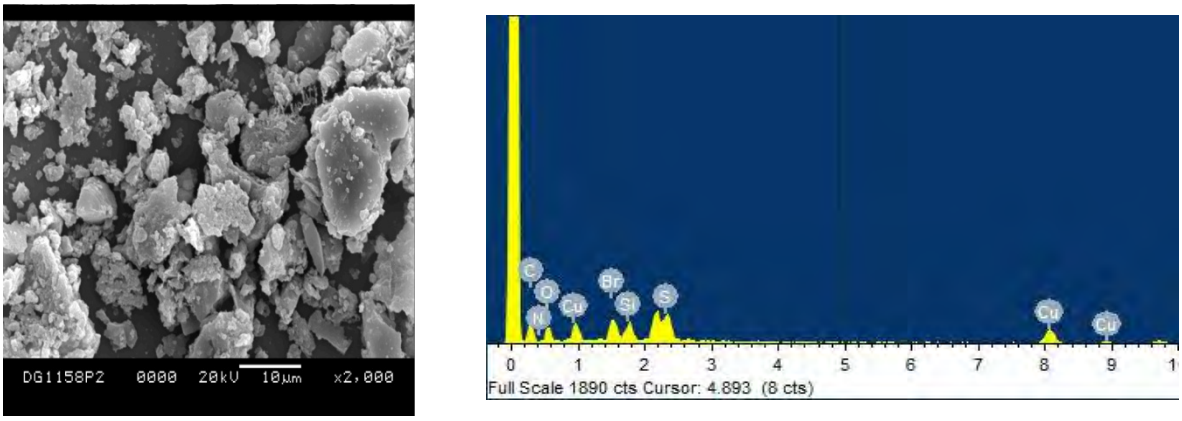

Fig S58: a) SEM image of Cu^{2+} coordinated Polymer **P2** film on quartz plate, b) EDX analysis of Cu^{2+} coordinated polymer **P2.**

References:

1. J. R. Lakowicz, *Principles of Fluorescence Spectroscopy*; Plenum: New York, 1999; Vol. 2.
2. D. F. J. Arago, and J. B. Biot, *Mem. Acad. Fr.* 1806, 7.
3. A. Chakraborty, D. Chakrabarty, P. Hazra, D. Seth, N. Sarkar, *Chem. Phys. Lett.* 2003, **382**, 508.
4. (a) IUPAC Commission on Spectrochemical and Other Optical procedures for Analysis, *Pure. Appl. Chem.*, 1976, **45**, 107;(b) Y. Chen, C. Zhu, J. Yang, J. Li, Y. Jiao, W. He, J. Chen and Z. Guo, *Chem. Commun*, 2012, **48**, 5094.